EVALUATION OF EFFECT OF ANATOMIC LOCATION ON ARTEFACT FORMATION DUE TO DENTAL IMPLANT IN CBCT - A RETROSPECTIVE STUDY

Dissertation submitted to

Maharashtra University of Health Sciences, Nashik

in the partial fulfillment of regulations

for the award of the degree of

MDS

IN

DEPARTMENT OF ORAL MEDICINE & RADIOLOGY

BRANCH IX

2022

CONTENTS

LIST OF TABLES

LIST OF GRAPHS

LIST OF FIGURES

LIST OF COLOUR PLATES

ABBREVATIONS

CBCT	Cone beam computed tomography
FOV	Field of view
kVp	Kilovoltage peak
mA	Milliampere
GV	Gray value
VOI	Volumes of interest
ROI	Region of interest
ΔGV	Mean gray value
ΔGVs	Gray value difference
MAR	Metal artefact reduction
MART	Metal artefact reduction tool
MRI	Magnetic Resonance Imaging
CT	Computed Tomography
CNR	Contrast to noise ratio
ERBBS	Epoxy resin based bone substitutes
SD	Standard deviation
MDCT	Multi Detector Computed Tomography
MSCT	Multi-slice computed tomography
PMMA	Polymethyl methacrylate
K2HPO4	Dipotassium phosphate
DICOM	Digital Imaging and Communication in Medicine
VRF	Vertical root fracture
Ti	Titanium
Zr	Zirconium
Pb	Lead
Al	Alluminium
ZrO_2	Zirconium dioxide

Au	Gold
Co	Cobalt
Cr	Chromium
%	Percentage
Ht	Height
Wid	Width
SD	Standard deviation
HU	Hounsfield Unit
Con	Concentration
Nos.	Number
Vol.	Volume
Sen %	Sensitivity
Spe %	Specificity

INTRODUCTION

In recent years, CBCT has become an imaging modality of choice in dental implantology, as it minimizes the limitation of 2 dimensional images such as geometric distortion and superimposition produced by periapical radiography[1,2,3]. It is an advanced imaging modality with an increased application in dentistry because of its high resolution to produce 3 dimensional image, diagnostic accuracy, linear measurement precision, shorter scan time, low radiation exposure, compact size and low cost as compared to that of CT[4].

It is widely used in dentistry, for pre and post-operative evaluation of dental implants and its surrounding anatomical structures[5,6]. In pre-operative phase, it is used to provide accurate information about height, width, quality and quantity of alveolar bone before implant placement while in post-operative phase, it is used to evaluate the signs and symptoms of peri-implantitis and to access marginal bone level

and bone implant contact[7]. However, in post operative cases, the presence of already placed implants produces metal artefacts in the CBCT images.

Metal artefact formation is one of the most common problem faced in CBCT images[8]. These artefacts are structures visualised in the image which do not actually exist[9]. They degrade the quality of images and makes them unusable for diagnosis[10]. They increase the time of interpretation by covering important anatomical structures in the area of interest and decreases their diagnostic accuracy[11].

Dental implants are made of different metals such as titanium, zirconium, and titanium-zirconium alloy. An implant being a high density metal, leads to formation of artefact due to variation in attenuation and absorption of x rays that results in beam hardening[12, 13]. The artefacts in CBCT image appears as a hyper dense linear streak reflected from object with high density associated with hypo dense area scattered between them[12,14,15]. While passing through the dental implant, the image is formed from high density photon by increasing the average energy of beam of X ray and by modifying reconstruction process of CBCT. The most probable cause for artefact formation can be absorption of low energy photons by the metal instead of high energy photons[12,14,16]. If post surgical follow up is attempted, the metal artefacts produced by dental implant decreases the tomographic image quality due to extreme variations in gray value around the metal structure and thus affect the post surgical evaluation of osseo-integration and peri-implantitis[2.17,18]. The artefacts appear more pronounced when multiple metallic objects are present.

Now-a-days, CBCT is practiced widely in dental implantology. Therefore, being a radiologist it is important to have adequate knowledge about the artefacts

caused by different exposure parameters in different bone densities to avoid unnecessary exposure of patient. In order to improve the quality of image, it is important to understand the exact cause and methods to improve or prevent formation of artefacts by using different metal artefact reduction softwares.

On reviewing the available literature, it revealed that very few in vivo studies have been conducted on metal artefact quantification produced by titanium dental implants using CBCT[2]. Equally, inadequate data is available among the Indian studies on the metal artefacts formation affected by anatomical site[2,3]. Therefore, this study was undertaken to evaluate the effect of anatomical location on artefacts formation caused by titanium dental implants using CBCT. In our study, most of the CBCT scans were present with titanium implants. The probable reason for getting maximum scans with titanium implants could be clinical efficiency, in terms of cost, success of treatment and minimal artefact formation.

AIMS AND OBJECTIVES

AIM

To evaluate the effect of anatomic location on the formation of metal artefacts produced by dental implants in CBCT.

OBJECTIVES

1) To quantify metal artefacts produced by dental implants in anterior and posterior region of maxilla and mandible using CBCT images.

2) To quantify metal artefacts at equidistant axial sections, from cervical to apical region of implant.

REVIEW OF LITERATURE

The introduction of CBCT device in dentistry has changed the way Oral and Maxillofacial Radiology is practiced, thereby allowing the dentist to diagnose in all the three dimensions[19]. Because of low radiation dose as compared to that of CT, its application has increased tremendously[20]. CBCT was embraced into the dental clinics very rapidly due to its high resolution to produce three dimensional image, diagnostic accuracy, linear measurement precision, shorter scan time, low radiation exposure, compact size and low cost as compared to that of CT[4,19].

Inspite of several advantages of CBCT as an imaging technique, there are few demerits. The most commonly observed problem in CBCT image is the formation of image artefact. In CBCT, the term artefact refers to "any distortion or error in the image that is unrelated to the subject being examined[4]." In the reconstructed CBCT image, the lack of uniformities in gray levels leads to artefact formation[21]. It can be

influenced by several factors such as type of implant material, kVp, type of CBCT machine, bone type, size of FOV, voxel size and anatomical site[8].

In dentistry, the dental implants are made up of different type of metals such as titanium, zirconium, and titanium-zirconium alloy. The artefacts in CBCT depend on the anatomic number and density of metal[22]. As the atomic number of Zirconium is high, as compared to that of titanium, more artefacts are produced with zirconium implants[23,24,25,26,27,28].

Lower kVp causes greater amount of beam hardening artefact in presence of dental implants in the CBCT images[8]. Therefore, use of higher kVp is recommended so as to decrease the production of artefact due to difference in the attenuation between the lower and higher energy beam caused by high density object[9].

So far in the literature, different types of CBCT machines such as Picasso Trio, ProMax3D- Planmeca, 3 D Accuitomo, OP300 Maxio have been compared to evaluate the influence of CBCT machines on the artefact formation. It has been observed that among the above mentioned CBCT machines, OP300 Maxio produced least artefact in the presence of dental implant followed by Picasso Trio and Accuitomo when gray scale measurements were considered[8,9,25,29].

The artefact produced by dental implants impairs the visibility of bone thereby making it difficult to assess[30]. Different studies evaluated the artefact formation in spongy and cortical bone[29,31]. In spite of having similar histologic features, spongy bone differs from cortical bone as it has interconnected cavities, which reduces its density, while cortical bone is more mineralized and compact[32]. **Martin *et al.* [29]** in their study observed higher amount of artefacts in presence of cortical bone while

Shokri *et al.* [31] found greater amount of artifact in the cancellous bone. These variations in the results can be due to differences in the methodology as the wax better simulates the clinical conditions with heterogeneity and influences the gray value quantification in the region of evaluation, while polymethyl methacrylate phantom is homogenous[8,29,31].

Amount of artefact formation is directly proportional to size of FOV. Therefore, larger FOV generates greater amount of artefact as compared to smaller FOV. [8]As smaller voxel size decreases the quality of image and produces greater amount of artefacts, use of large voxel size is recommended[8].

Machado *et al.* [2] quantified the amount of artefacts according to the difference present between minimum and maximum gray value of similar CBCT machine and they noted no significant difference between the amount of artefacts between isolated and adjacent implants. They observed more number of artefacts in the anterior region of mandible and noted that variations in the gray value were influenced by the location and the adjacent anatomical structures[2].Similar findings were reported by **Oliviera *et al***.[3]who stated that same object might present variations in the gray value according to the anatomical sites, while **Valizadeh *et al.*[18]** noticed that position of object within FOV influences the grey value via the interaction of adjacent anatomical structure and X rays. Similarly, the effect of exomass explains the difference of artefacts according to anatomical sites[8].

Artefacts interferes with the diagnostic quality of CBCT images due to presence of metallic objects like implant, dental metallic restoration, post and core. These artefacts are caused due to high density of metal produced by beam hardening because

of difference in the attenuation and absorption of an X ray beam[12, 13]. In the CBCT image, they appear as alternating bright and dark streaks[33]. They impair the quality of images thereby making them diagnostically unusable and leads to improper diagnosis[33].

Artefacts in CBCT are broadly divided into 3 categories

1. Beam related artefacts
2. Patient related artefacts
3. Scanner related artefacts

Fig 1) Classification of artefacts:

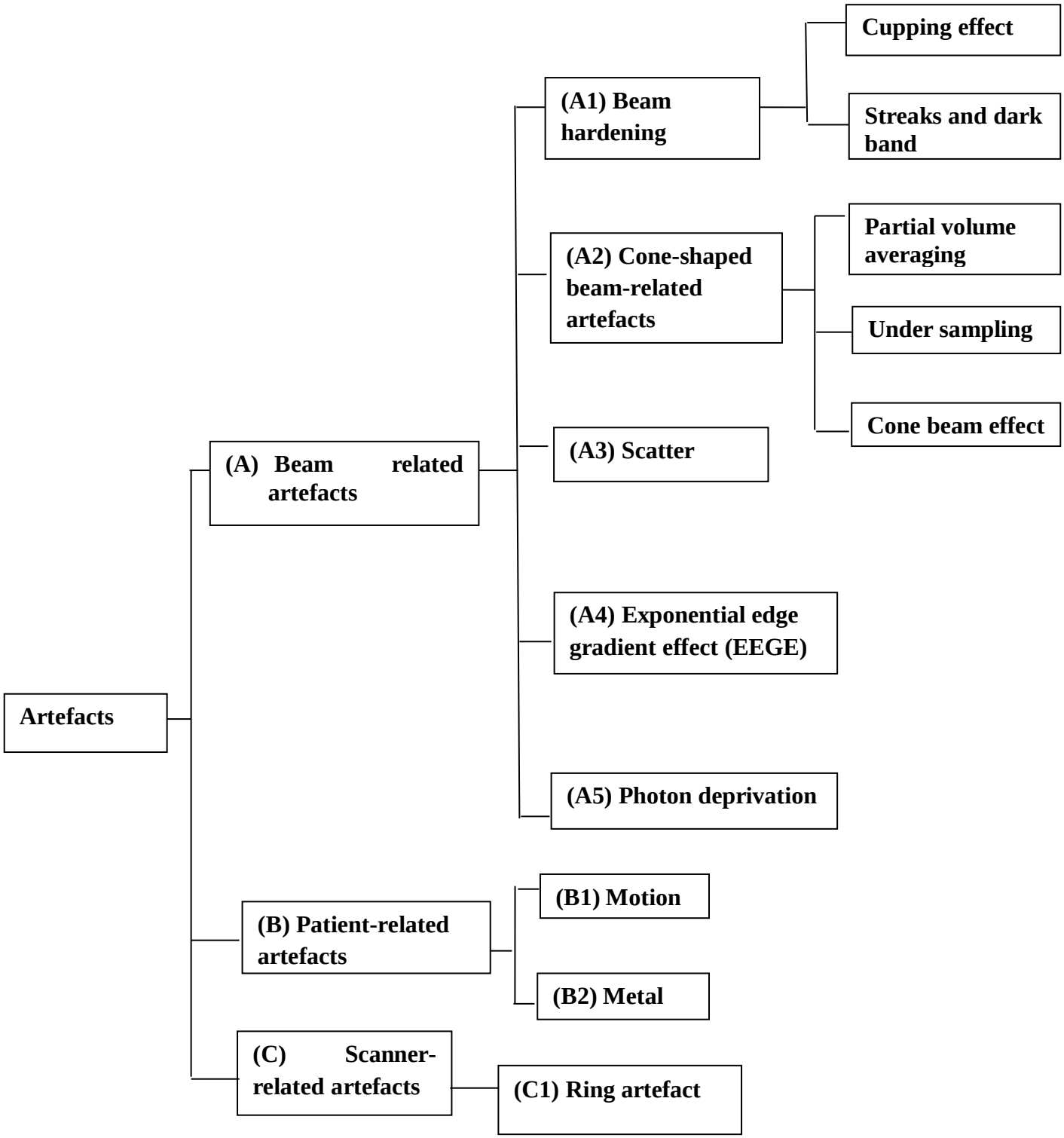

Classification of artefacts:

Beam hardening

It is the most common artefact seen in the tomographic images. An x ray beam containing individual photon has wide range of energy. When this beam passes through an object, photons with lower energy are absorbed instead of higher energy photons. Thus the beam gets "harder" and is called as beam hardening artefacts[34].It is further divided into 2 types:

I) Cupping artefact

II) Streaks and dark band artefact

Cupping artefacts

It occurs due to differential absorption caused by distortion of metallic structure**[1]**. It is observed while imaging a cylindrical object. When the beam passes through the centre of cylindrical object, it becomes harder as the beam has to penetrate through more amount of material present in the center of object than its edges. Thus, the beam becomes harder due to decrease in the rate of attenuation. Therefore, "saucer or cup" shape artefacts appear as a result of linear attenuation coefficient[34].

Streaks and dark bands:

They are found between 2 dense objects and create extinction artefacts. These artefacts are seen in 3D images and in axial planes between 2 dental implants that are in close proximity with each other**[34,35]**.

These artefacts can be prevented by reduction of fov, by modifying position of patient and by separating dental arches**[35]**.

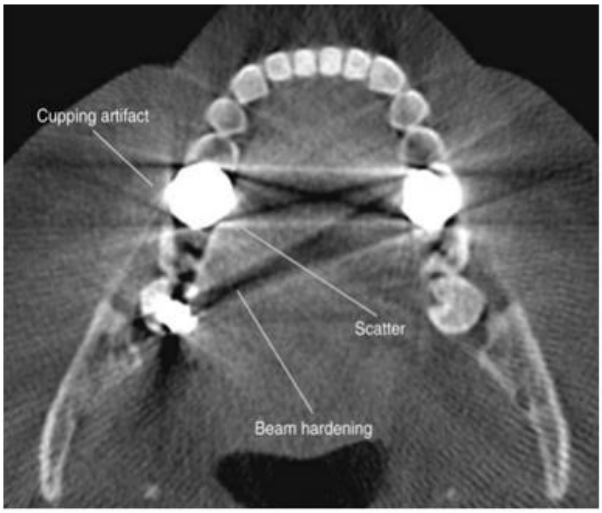

Fig 2) Axial view showing beam hardening (dark bands), cupping (image distortion) artifacts and scatter (white streaks). [1]

Cone-shaped beam-related artefacts

They include three types of artefacts:

a) Partial volume averaging

This type of artifact occurs when the resolution of voxel selected for the scan is larger than resolution of the object to be imaged. They are observed more frequently in areas where surface rapidly changes in thez- direction for e.g. in the temporal bone. Therefore, to reduce these artefacts it is recommended to select small and thin acquisition voxel[36].

b) Under sampling

This aliasing type of artefacts is formed due to incomplete rotational trajectory arcs or when sufficient basis projections are not provided for the image reconstruction. Decreased data sample leads to errors in registration, sharp edges and noisier image due to aliasing, which leads to formation of fine striations in the image. The importance of this artefact in context of diagnostic information, should be considered as the number of

basis projections or complete trajectory arch rotation is directly proportional to the patient exposure[4,36].

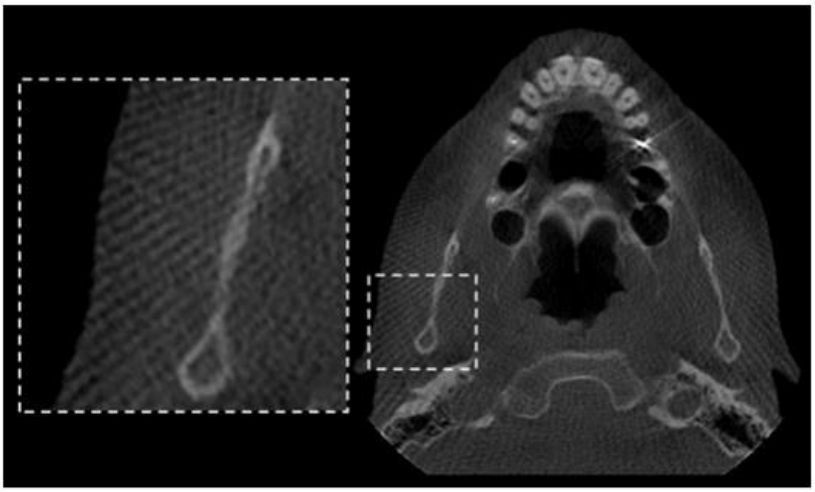

Fig 3) On the periphery of CBCT image, fine alternating hyperdense and hypodense stripes are seen radiating from the edge of the volumetric data, resulting in "Moiré" pattern, which is a type of aliasing artifact. [1]

c) Cone beam effect

Because of divergence of beam of X-rays, the cone beam effect is visible in peripheral portions of the scan volume which may lead to image distortion, streak artefacts and peripheral noise. This effect can be minimised by introduction of newer cone beam reconstruction by manufacturer. Similarly, it can also be minimised in clinical cases by affecting the ROI in the horizontal plane of the x ray beam[35].

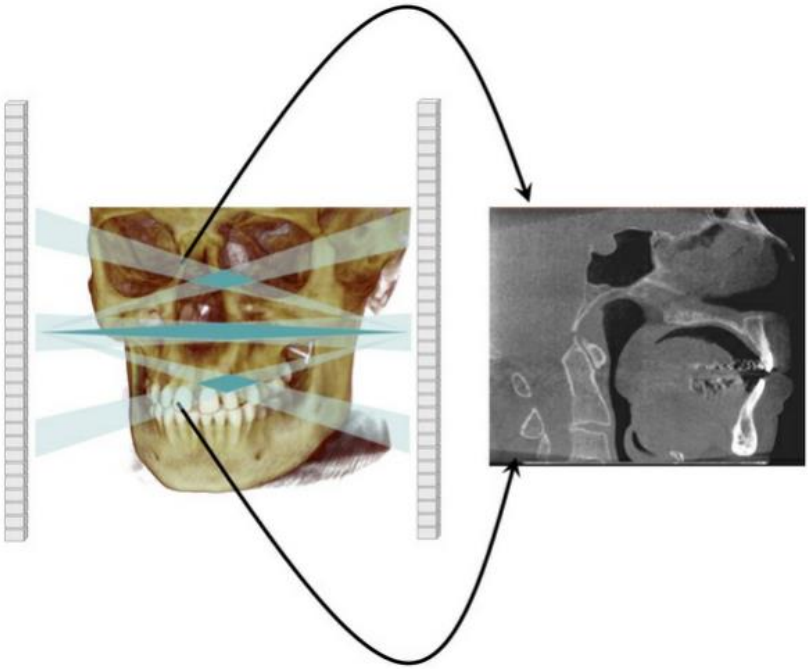

Fig 4) Showing schematic of Cone Beam Artifact. Exaggerated projection of three representative x-ray beams (one perpendicular, one angled inferiorly, and one angled superiorly) from the focal spot point of origin is shown at two positions of the x-ray tube rotation, 180 degrees apart. The optimal amount of data collected by the detector for reconstruction corresponds to the solid blue volume between the overlapping projections. Centrally, the amount of data acquired is maximal, whereas peripherally (transparent blue), the amount of data collected is appreciably less. The midsagittal section image demonstrates the visual effects of data interpolation by the reconstruction algorithm owing to inadequate data obtained at the peripheral superior and inferior extensions of the volumetric data set producing a peripheral "V" artifact of increased noise, distortion, and reduced contrast[1].

Scatter

This type of artefact occurs by diffraction of x ray photos from their initial path after it interacts with matter. The photons which are scattered are responsible for causing image degradation or quantum noise is captured by area detector of CBCT. It produces streak artefacts which are similar to the artefacts produced by beam hardening[21].

Fig 5) Quantum Noise Cone Beam Computed Tomography (CBCT) Artifacts. Axial high-resolution CBCT image at default resolution showing marked graininess caused by contamination of detector signal by scatter radiation [4].

Exponential edge gradient effect

It occurs when high contrast to the neighbouring structures is produced by borders of metallic crown with sharp edges. It produces streaks in the direction of projection which are perpendicular to long straight edges[35].

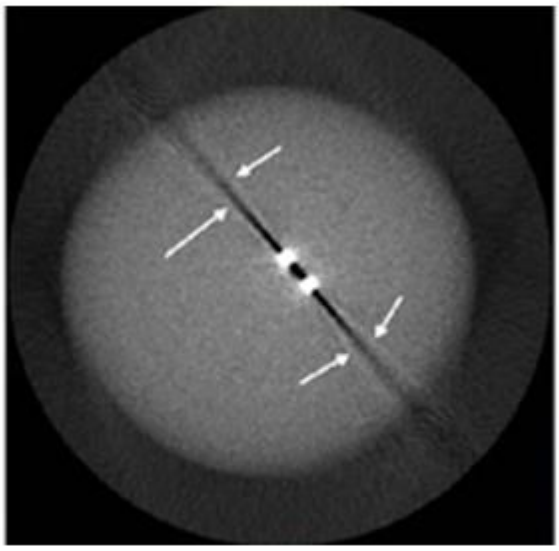

Fig 6) EDGE with thin line tangent to sharp edges (arrow) in the direction of the beam[9].

Photon deprivation

Severe beam hardening leads to photon deprivation and are usually observed adjacent to titanium implants or heavy metal restorations. When sufficient photons does not reach the detector, due to high density of metallic restorations, a complete void exists in the image, and appears like a pseudo fracture on the axial images. This is known as photon starvation[35].

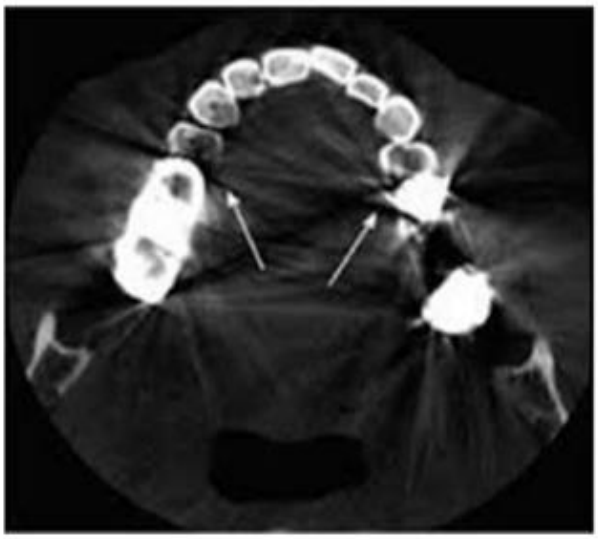

Fig 7) Arrows showing photon deprivation[36].

Motion artifact

Patient movement leads to faulty or mistsregistration of data in the reconstructed image. Artefacts due to these movements are frequently observed in CBCT due to long acquisition time as compared to that of conventional radiography. These artefacts may be ascribed to improper patient stabilization thereby causing double contours and blurred image in the reconstructed image which results in poor quality images. High resolutions of the present CBCT ranging from 0.08 mm - 0.4 mm may cause a detrimental effect on quality of image even on small movements. Therefore to minimise these artefacts, head restrainer and shorter scanning time should be used[15].

Fig 8) Arrow showing typical double contours produced by patient movement[9].

Metal artefacts

These artefacts are also called as white streaks. Presence of metallic objects in area of scanning leads to severe streak artefacts. Density of the metal beyond the normal range may lead to incomplete attenuation profiles. Dense metallic structures such as crowns, dental fillings, surface restorations, implants, and surgical plates or screws degrades the image quality by blocking the X ray beam. Therefore, to minimise these artefacts patients are always advised to remove the metal objects like jewellery prior to scanning. However, gantry angulation may be practised to keep away the metal inserts such as dental fillings, prosthetic devices, and surgical clips etc from scans of nearby anatomy. These artefacts can be minimised with the help of MAR software[11].

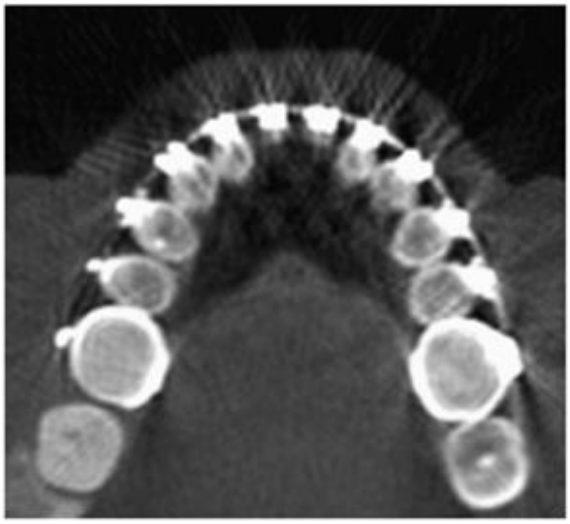

Fig 9) Metal artifact streaks from orthodontic bracket[37].

Scanner related artefacts

Ring artifact

They appear at the centre of axis of rotation as circular or concentric rings. It is caused due to defect in the scanner detector and error in calibration. Due to consistent and repeated readings at every angular placement of the detector, this artefact results in ring or circular shape. Presence of this ring shaped artefact indicates the need for recalibration or repairy of detector. This type of artefact is quite uncommon now a days as all the modern scanners uses solid state detectors[4].

Fig 10) Arrow showing Ring artifact[4].

Artefacts are frequently encountered in CBCT and their presence affects the clinical judgment of the dentist[32].Therefore, it is necessary to have a thorough knowledge about the artefacts affected by different exposure factors such as kVp, mA, fov, voxel size, implant material, bone and CBCT type so as to avoid unnecessary exposure of the patient[8].In order to improve the quality of CBCT image, it is important to understand the exact cause and methods to improve or prevent the formation of artefacts.

Review of literature on CBCT artefacts around dental implants and its associated factors.

Pauwels *et al.* (2011)[14] quantified artefacts of metal acquired from a varied range of CBCT machines and exposure protocols in order to compare their tolerability to various metal densities.They fabricated PMMA containing Ti and Pb rods and scanned them on thirteen CBCT machines and 1 MSCT machine, containing higher and lower dose exposure protocols. Artefacts from the Ti and Pb rods were measured by 2 experienced observers by quantifying the SD of voxel values present near the metal rods and by converting this value to % of theorotical maximum SD. They observed that in CBCT, values of artefact varied from 6.1% to 27.4% for Ti, and from 10.% to 43.7% for Pb. Most of the CBCT machines performed worst on comparison to that with MSCT for Ti artefacts, but each of them presented well for Pb artefacts. Overall, they noted no difference in the metal artefacts for higher dose protocols, though few machines exhibited less reduction in artefact for larger field of view or higher exposure protocols. They concluded that areas neighbouring the metal rods were moderately affected, mostly in areas in between Ti and Pb rods.

Cremonini *et al.* (2011)[1] evaluated the effect of metallic artefacts on the location of implant using MSCT and CBCT Technique. They scanned 10 mandibles twice by both the techniques, with and without dental metallic artefacts. They placed metal restorations on the tip of the alveolar ridge near the mental foramen before the 2nd scanning. Linear assessments i.e wid. and ht for every cross-section was carried out by a single observer and each mandible was examined at both the right and the left region of mental foramen. They observed that the dental metallic artefacts produced 5% increase in bone thickness by multislice and 6% increase by CBCT technique. There

was 6% and 0.68% reduction in bone height by multislice and CBCT technique respectively. Both the techniques did not show any significant difference in measurements performed with and without metallic artefacts though its existence made the position of the crest of alveolar bone more difficult.

Chindasombatjaroen *et al.* (2011)[16] compared the artefacts caused by metals in CBCT and MDCT machine with respect to type of metal and imaging parameters. They conducted a study on blocks of Al, Ti, Co-Cr and type IV Au alloy and examined them under CBCT and MSCT scanner at voltage of 80 and 100 kVp, 100 mA and 170 mA by Multi Detector Computed Tomography and 102 and 170 mAs by Cone Beam Computed Tomography. Areas of artefacts were measured by using Image J software. They observed that areas of artifact for the similar metals and scanning parameters were lesser with Cone Beam Computed Tomography as compared to that in Multi Detector Computed Tomography in most of the conditions and Type IV Au alloy produced greatest area of artefact which was followed by Co-Cr alloy, Ti, and Al respectively. Greater tube voltage was related with lesser artifact in most of the conditions, while increased mA had no constant impact on the area of artefact area in both the CT machine. So they concluded that Cone Beam Computed Tomography was related with lesser artefact areas than with Multi Detector Computed Tomography for the similar parameters and Type IV Au alloy caused the greatest area of artefact between the tested metals, but metal artefacts can be decreased by raising the tube voltage.

Luckow *et al.* (2011)[38] conducted a study to enhance the quality of image in CBCT by tilting the mandible containing 2 dental Ti implants. They performed CBCT on the mandible, with varied voltage, beam current, rotation angle of the mandible and

the tilt angles of the mandible with reference to the source detector plane. The various datasets were registered with regard to data of micro CT for extraction of the common volumes and divergence from the pre-defined criteria which characterizes the quality of image. They noted différences in the accelerating kVp, mA and the rotation in the source-detection plane. They observed that quality of image improved by a factor of 2 when the mandible was tilted by 14°. They concluded that tilting mandible with two implants reduces the artefacts of the highly absorbing X-ray materials in the Cone Beam Computed Tomography images. They further mentioned that time of exposure and dose could be decreased by a factor of 4 without reducing the quality of image.

Bechara *et al.* (2012)[39] investigated if MAR algorithm was useful and improved CNR. They built a phantom embedded with 3 metallic beads and 3 EBRS to simulate bone adjacent to metal in the middle of the FOV and at the periphery. 10 data sets were obtained at 50–90 kVp and the scans obtained were examined using Image J software. Gray level variations were assessed using profile lines while contrast was assessed using area histograms. They calculated CNR. They observed that MAR decreased changes in GV and increased CNR. The GV variance was least when the phantom was placed in the center of the volume and the MAR was operated. The quality of image enhanced as the peak kVp was raised. They concluded that better quality images of a phantom were acquired when the MAR algorithm was used.

Bechara *et al.* (2012)[40] investigated if MAR algorithm of the Picasso Master 3D CBCT machine decreased the prevalence caused by metal artefacts and raised CNR while maintaining the similar GV in absence of metal body present in the scanned volume. They acquired twenty images within a range of 50–90 kVp. 10 of which contained metallic bead placed in the phantom. They used Image J software to analyze

the images. They evaluated the average GV variation of the ERBS and control area by using area histograms and calculated CNR. They observed that metal artefact reduction algorithm raised contrast to noise ratio when the metallic bead was present and improved the gray level of ERBS regardless of presence metallic bead. The quality of image improved as peak tube potential was raised. They concluded that use of metal artefact reduction algorithm in the existence of a metal bead improves the quality of images and regains the control gray values.

Esmaeili *et al.* (2012)[41] evaluated the nos of artefacts produced due to beam hardening in the scans of implants and compared them between 2 New Tom VG and Planmeca Promax 3D CBCT machines. For study, they used an implant drilling model and placed implants in the region of canine, premolar and molar and carried out scanning methods using 2 Cone Beam Computed Tomography machines. They evaluated coronal and axial sections containing implants and determined the nos of artefacts present in every image. They observed significant difference in the beam hardening artefacts in the axial and coronal views present between the 2 CBCT machines, with a greater quality of images obtained by the NewTom VG CBCT machine. They concluded that NewTom VG CBCT machine exhibits less beam hardening artefacts in comparison with Planmeca Promax 3D Max CBCT machine.

Benic *et al.* (2013)[17] evaluated the geometrical pattern and the severity of artefacts surrounding Ti implants in Cone Beam Computed Tomography. They used 10 models, containing Ti implant of 4.1mm diameter. In every model, implants were placed in one of the gaps of tooth: 37, 36, 34, 33, 31, 41, 43, 44, 46, and 47. They produced 3 models free from implants for control purpose and scanned each model for 5 times by using a Cone Beam Computed Tomography scanner. They recorded GV at 8

circular positions surrounding the implants at distance of 0.5 mm, 1 mm, and 2 mm from the surface of implant. They quantified GV in VOI in the models free from implants and calculated GV between the GV Test and GVControl. They observed that the artefacts which were reflected by modified gray value were always present near the Ti implants irrespective of their location. When GV_{Test} and $GV_{Control}$, were compared, the increased gray values were observed in the buccal and lingual surface of implant sites while region with decreased gray values were placed perpendicular to the body of mandible of test models. A statistically significant reduction was found in the severity of artifact with increased distance from the buccal implant surface. They concluded that artefacts surrounding Ti implants in CBCT scans were dispersed according to the geometric pattern.

Parsa *et al.* (2013)[42] evaluated variation in the GV at the site of implant with various parameters such as FOV, spatial resolution, nos of projections, time of exposure and selection of dose with the help of 2 CBCT machines and compared the outcome with those acquired from MSCT. They scanned partially edentulous mandible by using 3 Computed Tomography machines: MSCT and 2 CBCT machines i.e. Accuitomo and New Tom 5G®. They obtained 36 scans from the Accuitomo and 24 scans from the New Tom and converted them to DICOM 3 format and performed the data analysis using 3Diagnosys® software. One probe designating the site was inserted on the MSCT scan for the placement of pre-operative implant. The inserted probe on Multislice Computed Tomography was then converted to the same area on both the Cone Beam Computed Tomography image by using a vol. based 3 D algorithm. For each CBCT scan, the average voxel GV of the area surrounding the probe was derived individually and the impact of imaging parameters on the quantified average voxel GV were

evaluated. They noted significant difference in the gray values of both the CBCT systems from HU values quantified with Multislice Computed Tomography. Scan field of view and spatial resolution selected in both the CBCT systems showed a significant impact on the measurement of gray value. They observed a significant impact in the Accuitomo CBCT machine, due to number of projections selection but the exposure time and dose selection did not reveal any significant impact on the measurements of gray value in the New Tom CBCT machine. They concluded that the GV from Cone Beam Computed Tomography scans were affected by machine and scan setting.

Oliveira *et al.* (2013)[3] assessed the effect of anatomical site on the Computed Tomography numbers in mid and full field of view of CBCT scans. The images of CBCT in the areas of incisor, premolar, and molar dental sockets in the phantom of human skull filled in with tubes of polypropylene containing different concentrations of K_2HPO_4 were obtained using New Tom 3G and New Tom 5G CBCT machines. They measured Computed Tomography numbers of the dipotassium hydrogen phosphate phantoms and examined the association between Computed Tomography numbers and conc. of dipotassium hydrogen phosphate phantoms and compared measured Computed Tomography numbers of the dipotassium hydrogen phosphate phantoms present between the anatomical location. They found a strong linear association between the Computed Tomography numbers and dipotassium hydrogen phosphate conc. at all six anatomical locations but absolute CT numbers were found varying with anatomical location. They concluded that the association present between the Computed Tomography nos. and density of object was non- uniform throughout the arch on Cone Beam Computed Tomography images.

Naitoh *et al.* (2013)[43] assessed mesio-distal artefacts of metal produced from implants placed in the posterior region of mandible by using Cone Beam Computed Tomography machine. They included 22 individuals having sixty one implants placed in the posterior region of mandible and measured values of pixel around implants with the help of CBCT and OPG machine. They reported that the average values of pixel between dental implants, between dental implants and neighbouring teeth, and posterior to dental implants were remarkably lesser than in between neighboring teeth in Cone Beam Computed Tomography. However, the average values of pixels between the implants didn't significantly vary from that between the neighboring teeth in OPG. So they concluded that mesio-distal metal artefacts around implants were visible on the Cone Beam Computed Tomography.

Parsa *et al.* (2014)[44] assessed the utility of MART in the software of the OP300 CBCT machine for the improvement of GV levels in post-operative scans of implant. They selected total twenty implant position from five edentulous mandibles and scanned them with the help of CBCT machine and produced scans under 3 various conditions i.e implant sites drilled without implants, implants placed without MAR and implants placed with MAR. 3 images of each mandible were overlapped by using software. They derived the average GV of identical areas of bone surrounding the implants for every condition and assessed the variation between GV measurements taken from the location of the implant obtained from various conditions. They reported remarkable variation in the GV from the scans without implant and scans with implants. Similarly, GV across scans with and without metal artefact reduction did not show significant difference.They concluded that MART in the software of OP300 Cone

Beam Computed Tomography machine had no effect on the GV produced by artefacts of metal near the implant.

Oliviera *et al.* (2014)[45] assessed the impact of mA and kVp on the variations of CBCT voxel values. They obtained CBCT images from phantoms in different conc. of K_2HPO_4 under various parameters of mA and kilovoltage peak. The images were acquired with and without the use of dental implant and exomass. The variations of Cone Beam Computed Tomography voxel values were quantified. The relationship between variability in values of voxel and K_2HPO_4 conc. was assessed by using linear regression. The mA and the existence of a dental implant had no effect on the variability of voxel values. Scans performed at the high kilovoltage peak value exhibited a considerable decrease in voxel value variability when exomass was absent. At the high levels of mA and kilovoltage, the variability in voxel value was not affected by exomass in images. The presence of exomass resulted in considerable decrease in the variations of voxel value in all the scans. Greater conc. resulted in higher variances in the voxel values in all scans, except for those operated at the greatest levels of mAs and kilovoltage. They concluded that current had no effect on the variations of Cone Beam Computed Tomography voxel values; but when the object was smaller than the FOV; greater kilovoltage peak resulted in decreased variations.

Pauchades *et al.* (2015)[23] conducted a study to evaluate the severity of artefacts surrounding Ti, Ti-Zr, ZrO_2 implants in Cone Beam Computed Tomography images. They used 20 human models of mandible, each consisting of at least 1 implant within the single-tooth gap position 45. They produced 5 test models for each type of implant : titanium of 4.1mm diameter, titanium of 3.3 mm diameter, titanium–zirconium of 3.3mm diameter and zirconium dioxide of 3.5- 4.5mm diameter of

implants and 3 models free from implants were used as control. These models were scanned using CBCT machine. The gray values at 8 ROI surrounding the implants at 0.5mm, 1mm and 2mm away from the surface of implant were recorded and evaluated VOI of gray value in the control human models free from implants. Variations in the Gray value between test and control human model were evaluated in %. The highest absolute values were recorded in ZrO 3.5–4.5mm which was preceded by titanium-zirconium of 3.3mm, titanium of 4.1 mm and titanium of 3.3 mm. Variations of GV between Zirconium dioxide of 3.5-4.5 mm and other group showed statistical significance in most of the VOI. There was no statistical significant difference in the gray value for implants of Titanium-Zirconium of 3.3 mm, titanium of 4.1mm and titanium of 3.3mm in most of the VOI. Positive gray values were detected in buccal, mesio-buccal, lingual and disto-lingual surfaces, while in mesial and distal surfaces negative values were identified. They concluded that ZrO_2 implants generated significantly greater artefacts than Ti and Ti –Zr implants. The severity of the artefacts surrounding ZrO_2implants showed average 3 fold on comparison with that of titanium implants.

Valizadeh *et al* (2015)[18] evaluated the impact of location of object in FOV of CBCT for determining VRF with intra canal posts. They obtained sixty extracted teeth of premolar and made a cut at the Cemento enamel junction level. To make space for intra canal posts, they removed coronal 2/3rd of the root canal filled teeth. They arbitrarily divided the teeth into 2 groups of 30. In group 1, Instron machine was used to induce fracture while in the control group no fracture was made. Five different positions were used to scan all the teeth starting from the centre of FOV and in right and left side and in anterior and posterior region with respect to centre. i.e. from 3, 9,

12, 6 O' clock position with New Tom VGI CBCT machine. The scans for vertical root fractures were assessed by 2 observers. They observed that probable Sen% was same in all the positions while the probable Spe % of center position was remarkably greater than 6 O' clock and 12 O' clock positions. Taking into consideration the parameter of diagnosis, the values of Sen% and Spe% reduced in every location of field of view while the centre position of field of view showed statistical significance than that of other location; with higher Spe%. at the 3 O' clock position. They concluded that, the centre position is preferable for detecting VRF in teeth with the intra canal posts because of greater Sen% at this position. In case of intact teeth without fracture the 3 O' clock position would be ideal for determination because of greater significant Spec. % at this position.

Panjnoush *et al.* (2016)[46] evaluated the impact of mA, kVp, type of metal and location of metallic objects on the formation of artefacts in CBCT images. They fabricated Ti and Co-Cr rods and inserted them in human mandible. Promax 3D CBCT machine with various mA and kilo voltage were used for scanning the sample. The Image J software was used to evaluate the artefacts induced by metal objects within 4 area of interest on every scan. 97% of the cases (P=0.046) indicated that there was decrease in the artefacts present in buccal aspect of the titanium and cobalt-chromium rods with higher kvp but the intensity of artefacts among the 2 metals were not affected. 93% of the cases (P>0.05) did not show any effect on the metal artefacts with increased tube current. More severe artefacts were produced by a Co- Cr alloy as compared to Ti. Artefacts present in the buccal aspect of anterior rods were more intense than with posterior rods. They concluded that the intensity of metal artefacts on CBCT scans were

affected by kVp,mA and type of metal and the location of metallic objects. They further stated that intensity of metal artifact depends mostly on the metal type.

Vasconcelos *et al.* (2016)[13] evaluated zirconium implant artefact production in CBCT images with various protocols. They inserted Zr implant in the edentulous mandible and obtained 20 images with ProMax3D unit ranging from 70-90 kVp, voxel size 0.32-0.16mm. They activated MART in half of the CBCT scans and an axial section through the middle region of implant was chosen for every dataset. They also measured gray values in 2 area of interest 1 near to and other away from the implant and calculated CNR. They observed that SD reduced with higher kVp when the metal artifact reduction tool was used. The CNR was significantly greater when metal artifact reduction tool was turned off except for less resolution with kilovoltage values more than 80. Selected MAR and higher kVp resulted in an complete decrease in artefact in scans obtained with less resolution. They concluded that artefacts caused by Zr implants on the images of CBCT can be controlled by using 90 kilovoltage peak at less resolution and by activation of metal artifact reduction tool.

Sinha *et al.* (2016)[36] described artefacts in CBCT. In this review, they presented a pictorial essay describing artefacts, their classification and causes along with different methods and softwares to prevent or suppress artefact formation thereby preventing inaccurate or false diagnosis.

Fakhar *et al.* (2017)[47] evaluated the effect of position of fixture and crown filling on the precision of linear quantification by using 2 CBCT machine. They inserted 6 implants in human mandible in 2 stages and obtained CBCT scans in every stage by using Alphard VEGA 3030 and Promax 3 D Max CBCT machine. The CBCT

images were taken again after placement of metallic crown. The alveolar ht and wid was measured by 2 observers using five radiopaque markers. Values of same measurements performed before placement of implant were compared by using T test. The impact of implant position on the precision of linear quantification were evaluated by applying linear regression test. They noted that effect of fixture and crown-fixture combination on the precision of linear quantification of ht and wid was significantly undervalued. They stated that metallic crowns had no remarkable impact on the quantification of bone height and width. They reported that Promax 3 D Max CBCT machine undervalued wid. of bone remarkably greater than the another CBCT machine. They found more precision in measurements in the region of canine as compared to the region of adjacent implants. They stated that metallic artefacts can give rise to undervalued measurements though it was not statistically significant in their study.

Queiroz *et al.* (2017)[48] evaluated the effectiveness of MAR algorithm in CBCT images of materials used in dentistry acquired with various FOV and voxel size. For study, 2 imaging phantoms made up of acrylic resin were used. Every phantom had three cylinders made of the similar dental material: Cu-Al alloy. Cone Beam Computed Tomography images were acquired individually for every phantoms by making use of the Picasso-Trio CBCT machine at four field of volume sizes and 2 voxel sizes. Every phantom was imaged using with and without MAR. Each scan image was assesed in the On Demand 3D software and noise of image was assessed as the SD of the GV of ROI surrounding the cylinders of dental material. They observed that metal artefact reduction remarkably decreased noisy image surrounding the dental materials, regardless of FOV and sizes of voxel. They concluded that effectiveness of metal artefact reduction was same for distinct FOV and sizes of voxel evaluated.

Smeet *et al.* (2017)[5] analysed and evaluated imaging artefacts induced by Zr, Ti and Ti-Zr implants in MRI, CT and CBCT. They performed MRI, CT and CBCT by embedding these implants in gelatin. For MRI, they plotted 'Line distance profile' to quantify the accuracy of determination of size while for CT andCBCT, 6 shells around the implant were defined each 0.5cm from the surface of implant and determined histogram tool for every shell. Ti, Ti-Zr caused large signal voids in Magnetic Resonance Imaging due to its high susceptibility. With little distortion artifact, Zr implants could be clearly defined. The MR signal was suppressed upto 14.1 mm from the surface of implant for Ti and Ti-Zr alloy. In Computed Tomography, Ti and Ti-Zr alloy produced little streak artefact in comparison with Zr in CT. Ti-Zr alloy produced more severe artefact than Zr and Ti in CBCT. They stated that patients with zirconium implants allow better image contrast in MRI and produce limited artefacts. The CT and CBCT scans were less affected by artefacts from Ti and Ti-Zr alloy implant on comparison with that of Magnetic Resonance Imaging. They opined that the variations in artefacts caused by various materials of implant and imaging modalities can aid in selection of implant material.

Codari *et al.* (2017)[49] compared the impact of various CBCT machines, materials of high-density and FOV on the expressions of metal artefacts. They customised 3 acrylic resin phantoms having Ti, Cu–AL alloy and amalgam and examined them on 3 CBCT machines using high-resolution procedures, similar size of voxel of 0.2 mm and various FOVs. After automatic registration of image, the similar ROI was defined for small and medium field of volume. They assessed the variation between the segmented and real volume of metal cylinders. The variations in the area between the segmented and the true axial section were calculated for every segmented

slice. The background artefacts were measured near the cylinder, at 3 varied extents. They observed significant variations in the measurements of volume for all the Cone Beam Computed Tomography machines and materials for both sizes of Field of view. The slice per slice area analysis revealed increased artefacts along the metal cylinder′s edges and within materials, amalgam and Ti exhibited least and best artifact expression in every Cone Beam Computed Tomography machines. SD values in every device were found to vary between the 3 extents. They concluded that for evaluation of various CBCT machines, materials of high-density and FOV should be taken into consideration.

Rabelo *et al.* (2017)[50] measured artefacts from various root canal filling materials in CBCT images obtained from various exposure parameters. They scanned total 15 single rooted teeth using 8 exposure parameters with 3 other root canal filling materials and one without any filling was used as control group. Artifact measurements were done by a experienced observer who estimated the values in central axial section of all the obtained images in fixed ROI using Image J software. Calculations were based on percentage of hyper dense artefacts, remaining tooth area, hypo dense and tooth area influenced by artefacts. Qualitative Analysis was done by 2 observers and scores were given as absence of artefacts (0); moderately present (1); highly present (2) for hypo dense halos and line and hyper dense lines. They observed that there were no significant association between the exposure parameters between the quantitative and qualitative type of analysis, while significant difference was noted in the quantitative analysis among all the studied filling materials. In context of hyper dense and hypo dense lines, they found no similarities among the control group in relation to the qualitative analysis. There was no statistical difference in fibre glass posts from the

control group in relation to hypo dense halos. They concluded that various exposure parameters didn't influence objective or subjective examination of artefacts in CBCT images while the filling material used in endodontic restorations had no impact on both the types of measurements.

Sheridan *et al.* (2017)[51] evaluated the effect of implant induced artefacts on the precision of measurement of periimplant bone dimensions. They placed 19 implants in nine cadaver and took Cone Beam Computed Tomography images. They removed implants and took second image. The dimensions of implant and peri-implant bone quantification were determined. They reported no remarkable difference between the dimensions of implant or measurement of thickness of bone on every scan and significantly correlated thickness of bone at the platform and apex of implant. They concluded that existence of dental implants had no effect on the precision of CBCT measurements of thickness of bone caused by metallic artefacts.

Machado *et al.* (2018)[2] quantitatively compared the metal artefacts caused by titanium dental implants in different regions of maxilla and mandible on CBCT images. For study, they included a total of 200 implants from CBCT device and equally divided them into 4 groups. Group 1 included implants placed in anterior maxilla while group 2 included implants placed in posterior maxilla. Group 3 included implants placed in anterior mandible while group 4 included implants placed in posterior mandible. They further classified the implants into isolated and adjacent implants. They selected axial sections of every implant at apical, cervical and middle level and counted the amount of artefacts caused by implants on each slice. They observed that more number of artefacts were observed in the mandible as compared to maxilla and anterior region produced greater artefacts than the posterior region. They noted no significant difference in the

number of artifact between the isolated and adjacent implants and cervical level showed maximum number of artefacts. They concluded that metal artefacts are always produced in images of CBCT due to presence of dental implants and that these artefacts are influenced by anatomical location in CBCT.

Freitas *et al.* (2018)[52] evaluated the effect of kilovoltage peak and MART on the magnitude of artefacts of CBCT. They inserted Ti and Zr implants in the area of posterior mandible and CBCT scans were obtained with ProMax 3D and Picasso Trio machines by using 70,80 and 90 kilovoltage peak and by using with and without metal artifact reduction. The exposure parameters were set at 5mA, fov 80 x 50 mm and voxel size of 0.20mm and scans were done before and after placement of implants. ROI were selected at various extents from the artifact production area at 15mm, 25mm and 35mm in an axial scan, in which the standard deviation of GSV and CNR were measured. They observed that the MAR tool was efficient in reducing S.D. values when the artifact was pronounced. The CNR of Promax images were improved by MAR tool, but it did not affect the Picasso images. Furthermore, contrast to noise ratio was directly related with kVp tool in both the machines under study. They concluded that in both machines, increased MAR and kVp were effective in decreasing the CBCT artefacts.

Fontenele *et al.* (2018)[25] evaluated the amount of artefacts associated with Ti and Zr implants at various distances and angulations and studied their effect on the quality of CBCT images. They acquired images of CBCT before and after placement of Ti and Zr implants in the jaw on Picasso Trio, ProMax 3D and 3D Accuitomo 80 CBCT machines. They assessed artefacts by quantifying the SD of GV and CNR of 11 ROI at various distances of 1.5 cm, 2.5 cm and 3.5 cm and angulations of 65°, 90°, 115° and 140° from region of implant. They observed that SD values for scans

containing Ti did not vary from those of scans with no implant in all region of interest, but, greater values were noted in region of interest near the implant in Picasso. Zirconium images for Picasso and ProMax exhibited greater standard deviation values than the others in few region of interest. In ProMax, the variations could be seen even in the farthest region of interest from the implant. In Picasso, CNR were unaffected by the region of interest however the lesser values were observed in region of interest nearer to the Zr implant were recorded for ProMax and Accuitomo CBCT machines. They concluded that type of implant and CBCT unit influences the amount and magnitude of artefacts in Cone Beam Computed Tomography.

Kocasarac *et al*. (2019)[24] evaluated artefacts produced by Zr, Ti and Ti- Zr implants on the MRI, CT, and CBCT machines. 3 phantoms prepared from Zr, Ti and Ti- Zr implants were embedded in an ultrasonic gel. Different settings were used to obtain MRI, CT, and CBCT images. In Magnetic Resonance Imaging, the term artifact was considered as the length of signal void beyond limit of the implant and in CT and CBCT, the artefacts were obtained by deducting the dark level of picture element from the level of light picture element. They observed that Zr implants showed few distortion artefacts in MRI whereas Ti and Ti- Zr alloy produced severe artefacts. Artefacts in CT and CBCT, produced few artefacts with Ti and Ti-Zr implants than Zr. They observed least severe type of artefacts in Ti grade 5 implants with 0.3 and 0.4 mm voxels. They concluded that images of MRI were not much influenced from the artefacts caused by Zr implants while artefacts from Ti and Ti-Zr alloy implants were less severe in CT and CBCT images. CT generated more artefacts than CBCT and CBCT with large voxel sizes reduced dose-area product and artefact intensity.

Shokri *et al.* (2019)[31] assessed the impact of exposure parameters of Cone Beam Computed Tomography on the artefacts of metal caused by implants placed in various densities of bone**.** For study, they assessed total 27 blocks of bone with various densities, 9 of which were type 1, 9 were types 2 and 3, and 9 of which were type 4 and placed them in wax models of mandible and imaged them after drilling and after placement of implant using Cranex3D CBCT machines with a 4 × 6 $cm^2$and 6 × 8 cm^2field of view and 4 and 10 mA. They recorded GV of the blocks of bone before and after insertion of implants and observed that regardless of density of bone, the quantity of artefacts were less in smaller field of view on comparison with larger field of view while variations in current had no impact on metal artefacts and artefacts present in type 4 of bone were higher on comparison with that in other types of bone. Variations between type 1,2 and 3 were non significant. So they concluded that the quantity of artefacts in type 4 bone was greater than that in other types. FOV size and density of bone affected the metal artefacts surrounding dental implants; therefore a small FOV can be used to decrease metal artefacts.

Akay *et al.* (2019)[53] evaluated the prevalence of different artefacts or errors in the CBCT images and investigated the association between artefacts and variable such as age groups, sex, areas of imaging and time of acquisition. They evaluated five various types of artefacts and recorded age of patient, sex, cause for CBCT evaluation, the field of view, time of acquisition, anatomic region and existence of artefacts. They noticed beam hardening as the most commonly reported artifact and the number of artefact increased as FOV and voxel size increased.They noted 0.7% prevalence of motion artefacts and reported a statistically significant result between age and motion artefact and correlated cupping and aliasing type of artefacts within the FOV. They

concluded that artefact is an important issue influencing the quality of image so cautious patient posture and the optimal selection of scan parameter is an essential aspect in avoiding artefacts in CBCT image.

Safi *et al.* (2019)[54] introduced a novel method in CBCT for decreasing the metallic artefacts in the region of anterior teeth.In this technique, the patients were asked to puff out their cheeks during the rotation of x-ray tube. Images taken by this method were then compared with normal image and observed that metal artefacts near restored anterior teeth remarkably decreased. So they concluded that application of puffed-out cheek technique can considerably reduce the metal artefacts of CBCT scans from anterior region of teeth with metallic posts and crowns thereby leading to more accurate endodontic diagnosis.

Fakhar *et al.* (2020)[26] evaluated imaging artefacts produced byTi, Zr, and Ti-Zr abutments in CT, CBCT, and MRI.They placed 4×8 mm Ti fixture in thehuman mandible.Ti, Zr, and Ti-Zr abutments of size 10.5 mm were placed on the fixture one after the other. All abutment were imaged four times by every imaging technique. The GV of the images were recorded by 2 reviewers using the Image J software in 4 defined areas close to implant′s distal, mesial, buccal and lingual surface as the ROI. ΔGVs between the control i.e. fixture without abutment and case i.e. fixture and every type of abutment images were determined. They observed that in CBCT, ΔGV was remarkably greater in images of Zr-Ti, on comparison with the images of Ti abutments. In the distal, mesial, and buccal surface of region of interest in Computed Tomography, the ΔGV was greater in images of Zr than with titanium abutments. In the Magnetic Resonace Imaging, ΔGV for Zr was less than those for Ti-Zr and Ti samples. No remarkable changes in ΔGV were recorded between protocols of T1 and T2. They

concluded that Ti abutments created very few artefacts in the scans of CT and CBCT and artefacts wereminimal around Zr abutments in Magnetic Resonace Imaging.

Kocasarac *et al.* (2020)[27] evaluated the impact of artefacts caused by implants in the region of exomass on the Cone Beam Computed Tomography images. They assessed Ti, Ti – Zr and Zr implants, 4x5cm and 8x5 cm field of view obtained from the Planmeca ProMax CBCT machine, using with or without MAR, at 80 and 90 kilovoltage peak. In every axial scan, 3 ROI of 3.6 x 12mm were identified and standardized for images as: region 1: close to dental implant; region 2: in the middle of dental implant; and region 3: far from the dental implant. SD was calculated from the region of interest of histograms and was used as the measure of artifact. They also evaluated the effects of size of FOV, type of implant material, MAR, kVp, region and their interaction. They observed that Zr implant caused the highest artefacts, accompanied by Ti- Zr and Ti implants, mostly in the region 1. 8x5 cm field of view produced higher artifact as compared to that by 4 x 5 cm field of view when an implant was placed. Moreover, size of FOV didn't affect the quantity of artifact when a Zr implant or no metal artifact reduction was used; 90 kilovoltage peak created lesser amount of artefacts than 80 kilovoltage, peak and metal artifact reduction reduced artifact in the 8 x 5 cm FOV only, at 90 kilovoltage, peak and in Zr and Ti –Zr implant.They concluded that implants present in the region of exomass generates notable artefacts and imaging parameters should be considered as they decrease artefacts in the existence of a Zr implant.

Martin *et al.* (2020)[29] evaluated the effect of artefacts produced by Ti onstructures of bone in CBCT images considering various locations and amount of metals present in the dental arch, with and without MAR. In the present study, a

PMMA was constructed having 8 holes to mimic mandible in the intermediate plate. 3 Ti cylinders were placed in various positions and quantities to evaluate various clinically related situations and to measure the effect of metallic artefact surrounding 5 cylinders of bone.Images were performed by 7 different methods in 2 CBCT machines. 8 ROI surrounding every cortical and trabecular bone were used to estimate GV and SD corresponding to the AE in the Image J software. Both the artefact expression as well as effect of metal artefact reduction was evaluated. They observed that in both the OP300 Maxio and Picasso Trio CBCT machines, MAR was remarkably significant only for the protocols E, and F.Protocol F i.e. 3 metals present on the neighbouring region of analysis revealed greater artefact expression on comparison with others. So they concluded that expression of metal artefact was greater when more objects of metal were placed in the neighbouring structures of bone.

Fontenele *et al.* (2020)[55] assessed if activated MAR algorithm affected the magnitude of artefacts in images of CBCT.For study, they obtained volumes with and without Zr implants in mandibular region, by using the OP300 Maxio CBCT machine with 3 modes i.e. without metal artefact reduction, with activated metal artefact reduction after acquisition of image, and with activated metal artefact reduction prior to acquisition of image were examined. They measured artefacts in terms of SD of GV. CNR in 6 ROI each with different distance i.e..from 10 to 35 mm, i.e. from the nearest to the farthermost and angulations from 70° to 135° from the area of implant. They observed that in acquisition without metal artefact reduction, the areas near the dental implant i.e. at 10 mm and 15 mm exhibited greater standard deviation and lesser contrast to noise ratio than the far region. When metal artefact reduction was activated (before or after), standard deviation values didn′t vary in the areas.The area near dental

implant exhibited a remarkably low contrast to noise ratio in the acquisitions without metal artefact reduction than whenactivated metal artefact reduction after the image acquisition; moreover, activating MAR before the acquisition had no difference from either of the condition. They concluded that both ways of MAR activation was succesful in reducing the amount of artefacts of CBCT mostly when the impact of the artefacts is more visible.

Vadhani *et al.* (2020)[22] compared the intensity of implant induced metal artefacts on the CBCT images. For study, they selected dry human mandible and maxilla and placed two Roxolid and Zirconium fixtures of different diameters in the central incisor, first molar sockets and fixed them in dental wax. The mandible and maxilla were then placed in the simulated phantom for soft tissue and the plane of occlusion was adjusted parallel to the horizon. Images were taken at standard and high resolutions using two CBCT units. The CBCT GV were measured in 3 longitudinal sections of the fixture i.e. at cervical, middle and apical level and calculated CNR. The Contrast to noise ratio values of images were analyzed based on the material of fixture, resolution, jaw, unit parameters and fixture size. They observed that depending on the CBCT unit, the CNR values in Roxolid and Zirconium fixtures were completely different. Under higher exposure parameters, the CNR values of the Roxolid and Zirconium fixtures were significantly higher in the maxilla than in mandible. However, the fixture size and longitudinal section had no significant effect on the CNR values. They concluded that in contrast to the fixture material, scanning parameters and jaw type, differences in the size and longitudinal section of the fixtures had no effect on the severity of artefact.

Min *et al.* (2020)[6] conducted a study to decrease inter-implant area of metal artefacts in CBCT by modifying the position of angle of subject with respect to the source–detector plane. For study, 2 implants were inserted in a cube of impression material. They scanned the specimen with a CBCT machine at 7 angles i.e. 0°, 15°, 30°, 45°, 60°, 75°, and 90° along the 3 varied spatial axes i.e. alpha, beta, gamma resulting in 21 experimental groups. 13 VOI included inter area and peri-implant regions chosen from every axial reconstruction right angled to the implants. GV of every picture in the volume of interest was quantified. Average variations in GV between the volume of interest and control area were determined and reported in %. These difference in gray values vary from the various spatial angle were compared and analysed. They observed that as α angle raised, the gray value difference of the inter-implant area raised from − 62.02% to 0 whereas the SD reduced. They noted that ΔGV increased remarkably with the alpha angle and volume of interest on the line of extension of 2 implants revealed same results. After the adjustment of beta and gamma angles, they reported no remarkable changes in ΔGV. They concluded that increasing angle of alpha can decrease the artefacts of metal present in the inter-implant area of images of CBCT.

Kim *et al.* (2020)[56] quantitatified MAR using the auto edge counting technique in CBCT. 4 customised phantoms with various dental prostheses such as amalgam, gold, porcelain-fused-metal and zirconia were scanned with and without the MAR. Various scanning parameters of 0.2 and 0.3 mm3 voxel sizes and 70 and 100 kVp were used. Using auto edge detection in MATLAB, the quantity of artefacts decreased by every prosthesis and scanning mode was automatically counted. The overall artefact reduction ratio was found to range from 17.3 per cent to 55.4 %. In comparison to the other prostheses, the Au produced the least amount of artefact. For

all prosthesis, MAR exhibited great performance in smaller voxel size mode. The MAR performance in a CBCT scan was effectively evaluated using automatic measurements. The MAR performance in CBCT image was efficiently evaluated using automatic quantification. They concluded that the influence of MAR varied depending on the type of prosthesis and imaging mode, implying that careful attention is needed when choosing a CBCT imaging method.

Shahmirzadi *et al.* (2021)[57] evaluated artefacts produced in CBCT from three dental implants by three MAR algorithm i.e. pre and post acquisition metal artifact reduction, and no metal artifact reduction by using settings of 2 kVp. Ti, Ti-Zr, Zr implants were inserted in the mandible. Images of CBCT were obtained by using 84 and 90 kVpat standard resolution for every three metal artifact reduction mode. Image J software was used to evaluate the images and to compute the severity of artefacts for every material and setting combination. They observed that applying no metal artifact reduction resulted in significantly more severe type of artefacts for the three materials of implant than either of the two metal artifact reduction algorithms; but there was no significant difference between pre as well as post-acquisition metal artifact reduction On average, the 90 kilovoltage peak setting produced less intense artefacts than the 84 kilovoltage peak. When compared to Zr, the Ti-Zr alloy produced substantially less intense artefacts. Ti produced artefacts at a intermediary level when compared to the remaining two materials of implant, although it was not statistically distinct from either. They concluded that use of Ti –Zr alloy at 90 kVp can reduce the artefacts with either setting of metal artifact reduction.

Terrabuio *et al.* (2021)[8] conducted an integrated review on various types of CBCT artefacts surrounding the dental implants and its associated factors. After

thorough search in the database, they included a total of 9 studies and observed that the beam-hardening artefact was the most commonly reported artefact around dental implant in CBCT and could be minimized with a small FOV, large voxel, and greater kVp. The factors that affected the production of artefacts were material of implant, type of bone, area of evaluation, extent, type of Cone Beam Computed Tomography machines, size of FOV, mA, kVp, and size of voxel. They concluded that the complication and advantage of these parameters in patients with implants should be taken into consideration.

Kocasarca *et al.* (2021)[28] compared the artefacts in CBCT derived from implants of various materials located inside FOV or in the exomass and to evaluate different imaging parameters to decrease them. They obtained CBCT scans of mandible having Ti, Ti-Zr or Zi implants. The scans were obtained by Planmeca Promax CBCT machines using FOV sizes of 8x5cm and 4x5 cm. They placed implants in the FOV of 8x5cm or in the exomass of 5x5cm. The scanning parameters used 3 conditions of the MAR i.e. disabled, low and high at 80 and 90 kVp. They acquired SD of GV of ROI. The material of implant, position of implant, MAR condition, levels of kVp and their interactions were analysed. They observed that Zr implants created highest SD deviation followed by Ti-Zr and Ti and noted that implants in the exomass generated images with greater SD values as compared to that of implants placed inside FOV. They stated that MAR was effective in reducing SD values mostly from the Zi implant, only when the implant was placed inside FOV and noticed that images with 80 kVp had greater SD values on comparison with 90 kVp. They concluded that implants in the exomass leads to greater artefact formation than when placed inside FOV.

Salemi *et al.* (2021)[58] assessed the effectiveness of MAR algorithm of 2 CBCT machines used for detecting peri implant fenestration and dehiscence. They placed 36 Ti implants in bone blocks of bovine ribs. Fenestration and dehiscence were produced in the buccal bone surrouding implants. CBCT scans were acquired by Cranex 3D and ProMax 3D CBCT machines with and without metal artefact reduction algorithm and images were evaluated by 2 experienced radiologists. The area under reciever operating characteristic curve, Sen%, Spe % and accuracy of various imaging modalities were quantified and evaluated They observed that in both the CBCT machines, use of metal artefact reduction algorithm reduced the area under the reciever operating characteristic curve and the diagnostic precision used for the detecting fenestration and dehiscence. They noted higher Sen%, Spe % and precision of CBCT machines without the use of the MAR algorithm. The Spe % of ProMax 3D CBCT machine for detecting fenestration was same for with or without the metal artefact reduction algorithm. They concluded that though Cone Beam Computed Tomography is useful for detecting peri-implant defects, the use of metal artefact reduction algorithm doesn′t enhance the detection of peri-implant fenestration and dehiscence.

MATERIALS AND METHODS

This retrospective and observational study was initiated after getting approval from the Institutional Ethical Committee. The study was carried out at private CBCT Center. Total 104 CBCT scans having dental implant placed in anterior and posterior region of maxilla and mandible were obtained from Orthophos SL CBCT Machine having 3 D Diagnostic software of 4.2 version.

Inclusion criteria:

CBCT scans having dental titanium implants with presence of prosthesis placed in anterior and posterior region of maxilla and mandible irrespective of patient's age and gender. In our study, most of the CBCT scans were present with titanium implants. The probable reason for getting maximum scans with titanium implants could be clinical efficiency, in terms of cost, success of treatment and minimal artifact formation.

Exclusion criteria:

1. CBCT Scans of implants placed in zygomatic bone.

2. CBCT Scans with restorations, crowns and metal post in proximity with implants.

Materials:

I) Armamentarium for CBCT scans

Orthophos SL CBCT Machine with 3 D Diagnostic software of 4.2 version having tube voltage of 85 kVp, tube current of 4-7 mA, and exposure time of second, field of view : 5x5, 8x8,11x11cm and 12 bit scale.

II) Armamentarium for determining gray scale values in CBCT scans

Image J software version 1.52a ,National Institute of Health, USA

Fig 11) Flowchart showing distribution of implants in study group and method of quantification.

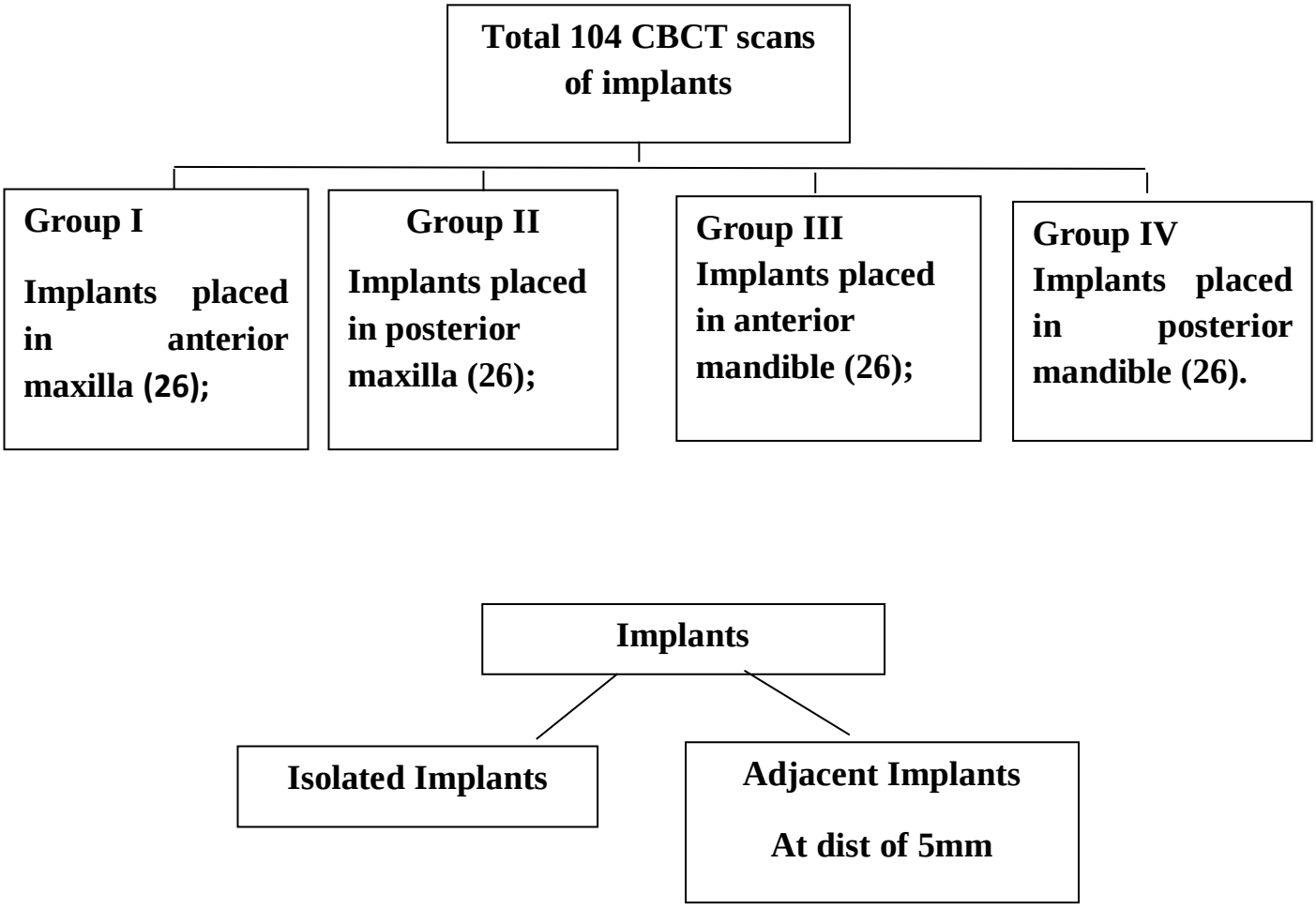

CBCT scans having titanium dental implants were obtained from Orthophos SL Sirona CBCT Machine.

↓

Axial scans of selected implants were subjected to further analysis.

↓

Area of interest with diameter of 10 mm around selected implant was marked with tool in the CBCT machine.

↓

Axial scans were analyzed by Image J Software

↓

The minimum and maximum grey values along with their actual standard deviation were determined using the histogram.

↓

Actual Standard Deviation $\xrightarrow{\text{Calculated as}}$ **Minimum & Maximum gray values obtained by Image J tool.**

↓

Theoretical Maximum Standard Deviation $\xrightarrow{\text{Calculated as}}$ **Half of gray value of CBCT machine.**

↓

$$\textbf{Formula: Artifact quantification (\%)} = \frac{\textbf{Actual SD}}{\textbf{Theoretical maximum SD}} \times 100$$

Methodology:

In the present study, total 104 CBCT scans with titanium dental implants placed in anterior and posterior region of jaw were obtained from Orthophos SL CBCT Machine with 3 D Diagnostic software of 4.2 version with acquisition protocol of 85 kVp, 4 to 7 mA, 27 sec rotation, FOV between 5x5 and 8x8 cm, 11x11cm and12 bit scale. According to inclusion criteria, total 104 CBCT scans were obtained and were equally divided into 4 groups according to the location of implant.

Group I —Included 26 Implants placed in anterior maxilla;

Group II —Included 26 Implants placed in posterior maxilla;

Group III —Included 26 Implants placed in anterior mandible;

Group IV —Included 26 Implants placed in posterior mandible.

The implants were further classified into isolated and adjacent implant. Too closely placed implants i.e. implants placed at a distance of 5 mm were considered as Adjacent implants.

Image selection

All the CBCT images were imported into DICOM software and each scan was evaluated at 5 different axial levels:

1. At cervical level
2. Between cervical and middle level
3. At Middle level
4. Between middle and apical level
5. At Apical level

Fig 12) CBCT image showing equidistant five axial levels from cervical to apical.

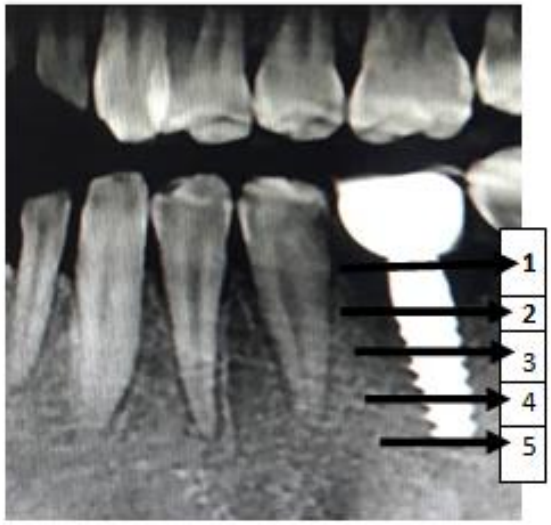

1. At cervical level
2. Between cervical and middle level
3. Middle level
4. Between middle and apical level
5. Apical level

1. Cervical level was defined as the level which enabled the visibility of superior or crestal end of implant.
2. It was defined as the level between cervical and middle level.
3. Middle level was defined as the midway between apical and cervical level.
4. It was defined as the level between middle and apical level.
5. Apical level was defined as the level which enabled the visibility of apical end of implant.

Quantification of metal artefacts in CBCT:

Image J Software version 1.52a, National Institute of Health, USA was used for the evaluation of axial scan selected for each implant.

In the software, area of interest with a diameter of 10 mm was selected by keeping implant as a centre.

Figure 13) Showing Area of interest with a diameter of 10 mm with implant as centre.

This area of interest enveloped the entire area of implant along with surrounding bone tissue as shown in the above figure. The image was then analyzed by Image J Software and histogram was obtained.

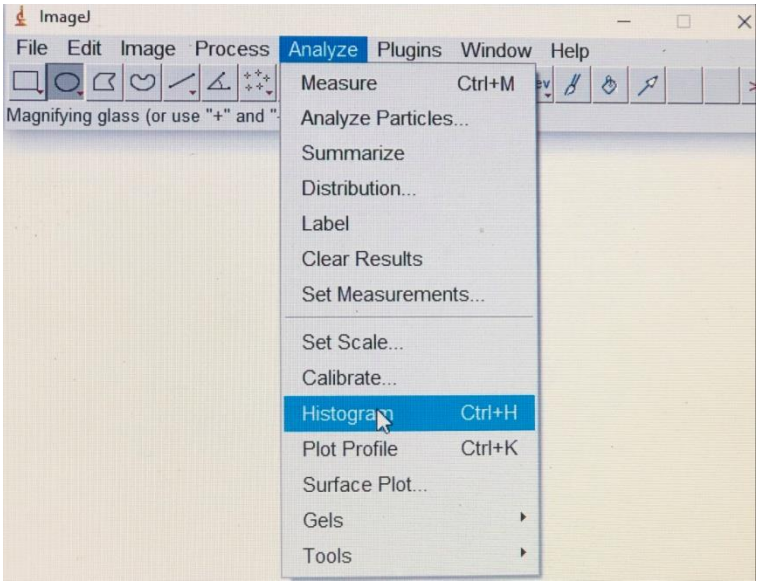

Figure 14) Showing Image J histogram software of version 1.52a.

The minimum and maximum grey values along with their actual standard deviation were determined using the histogram.

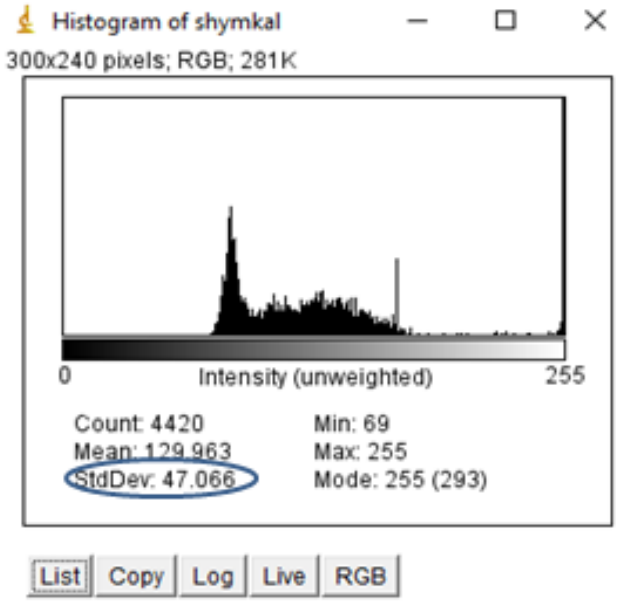

Fig 15) Showing histogram

The CBCT machine used in this study had 12 bit scale i.e 4096 grey values. From this value, the maximum theoretical SD was calculated, where theoretical maximum standard deviation corresponds to half the grey value of 12 bit image i.e. 2048 grey values.

Artefact quantification according to **Pauwels *et al* (2013)** can be defined as :

$$\text{Artefact quantification (\%)} = \frac{\text{Actual SD}}{\text{Theoretical maximum SD}} \times 100$$

Actual Standard Deviation $\xrightarrow{\text{Calculated as}}$ Minimum & Maximum gray values obtained by Image J tool.

Theoretical Maximum Standard Deviation $\xrightarrow{\text{Calculated as}}$ Half of gray value of CBCT machine.

Therefore, the Actual Standard Deviation was converted into percentage of the maximum theoretical SD, where higher percentage suggested more pronounced artefacts.

$$\text{Artefact quantification (\%)} = \frac{\text{Actual SD}}{\text{Theoretical maximum SD}} \times 100$$

STATISTICAL METHODS

The data on number of metal artefacts was obtained according to anterior, posterior, maxilla and mandible sites for isolated and adjacent implants and summarized in terms of mean, standard deviation and median. The comparison of median artefacts between different paired categories was performed using Mann-Whitney U test, while across slice comparison was performed using Kruskal-Wallis test.

All the analyses were carried out in SPSS ver 26.0 (IBM Corp, USA) software and the statistical significance was tested at 5% level.

The brief description of methods used is as below:

1. Measures of central tendency

If x_1, x_2,…x_n are the observations on a random variable X, then following measures of central tendency can be obtained:

- **Mean** for a set of observations is given by

$$\bar{x} = \frac{1}{n}\sum_{i=1}^{n} x_i$$

- **Median**: It is the middle value of a set of values when arranged in the increasing order of magnitude.

2. Measures of dispersion

- **Standard deviation** for a set of observations in given by

$$s = \sqrt{\frac{1}{(n-1)}\sum_{i=1}^{n}(x_i - \bar{x})^2}$$

Where x_i = observation on each object

n = number of objects

- **Mann-Whitney U test**

The test is a non-parametric equivalent of Student's t-test for independent samples, when the assumption of normality is violated. It evaluates the null hypothesis that the two populations are the same against alternative that particular population has larger values than the other. It involves computation of a test statistics based on ranked series. The observations are ranked according to magnitude irrespective of the two groups. The steps involved are as under:

i) Add the ranks for observations from group 1.

ii) Since sum of all ranks equal N (N+1)/2, the sum of ranks in group 2 is total sum minus the sum of group 1.

iii) A statistic U is defined as:

$$U_1 = R_1 - \frac{n_1(n_1+1)}{2}$$

wheren_1 is the size of sample 1 and R_1 is the sum of ranks of sample 1. Equally valid formula for U is

$$U_2 = R_2 - \frac{n_2(n_2+1)}{2}$$

The smaller of U_1 and U_2 is for significance testing.

For large sample sizes (N> 30), U is approximately normally distributed, and the standardized value is given by

$$z = \frac{U - m_U}{\sigma_U}$$

where

m_U and σ_U are the mean and standard deviation of *U*. The significance of z can be obtained from normal probability tables. Here m_U and σ_U are given by:

$$m_U = \frac{n_1 n_2}{2} \qquad \sigma_U = \sqrt{\frac{n_1 n_2 (n_1 + n_2 + 1)}{12}}$$

- **Kruskal-Wallis test**

The test is a non-parametric equivalent of one-way analysis of variance for comparing three or more groups. It is used for testing if the samples originate from same or different populations. The procedure for determining significance of difference across groups using the test is as below:

i) The n_1, n_2, …,n_k observations from k samples are combined into a single series of size *n* and arranged in order of magnitude from smallest to largest. The observations are then replaced by ranks from 1 assigned to smallest observation to n assigned to largest observation. When two or more observations have same value, each observation is given a mean of the ranks for which it is tied.

ii) The ranks assigned to observations in each of the k groups are added separately to give *k* rank sums.

iii) The test statistic is defined as:

$$H = \frac{12}{n(n+1)} \sum_{j=1}^{k} \frac{R_j^{\,2}}{n_j} - 3(n+1)$$

where k is the number of groups; n_j is the number of observation in j^{th} group; *n* is the total number of samples from all the groups and R_j is the sum of ranks from j^{th} group.

iv) When there are more than 5 observations in one or more groups, H is compared with the tabulated value of χ^2 with *k*-1 degrees of freedom.

COLOUR PLATE NOS 1

Armamentarium used for CBCT Scans: Orthophos SL CBCT Machine with 3 D Diagnostic software of 4.2 versions.

COLOUR PLATE NOS 2

Armamentarium for determining gray values in CBCT scans: Image J software version 1.52a.

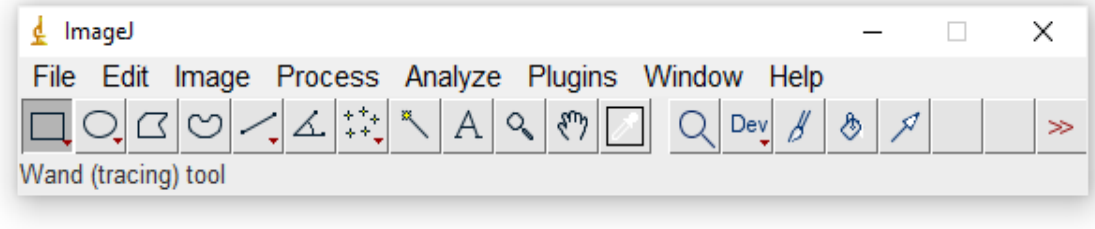

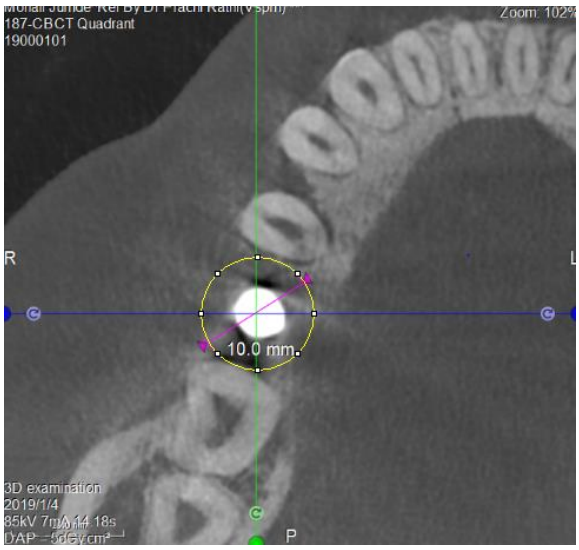

RESULTS AND OBSERVATIONS

A retrospective and observation study was undertaken to assess the effect of anatomic location on the artefact formation produced by dental titanium implant in CBCT. Total 104 CBCT scans containing titanium dental implants were obtained from private CBCT Centre.The implants assessed were internal hexagon within the length of 8 to14 mm and were equally divided into 4 group according to the location of the implant.

Group I —Included 26 Implants placed in anterior maxilla;

Group II —Included 26 Implants placed in posterior maxilla;

Group III —Included 26 Implants placed in anterior mandible;

Group IV —Included 26 Implants placed in posterior mandible.

The implants were further divided into isolated and adjacent implant.

All the CBCT scans was evaluated at 5 different axial levels:

1. At cervical level

2. Between cervical and middle level

3.Middle level

4.Between middle and apical level

5. Apical level

Image J Software of 1.52a version was used for quantifying the metal artefacts in percentage for the evaluation of axial sections for each implant.

Table 1: Provides distribution of dental implants in study groups

Out of total 54 isolated implants, 15 (27.8%) implants were present in anterior maxilla while 15 (27.8%) were present in posterior maxilla, 11 (20.4%) implants were present in anterior mandible and 13 (24%) implants were present in posterior mandible. There were total 50 adjacent implants, out of which 11 implants (22%) were present in anterior and posterior maxilla each, and 15 implants (30%) were present in anterior mandible while 13 (26%) implants were present in posterior mandible.

Table 2) Provides the comparison of metal artefacts in percentage between the anterior maxilla and anterior mandible.

No significant difference was observed in the percentage of metal artefacts produced by implants between the anterior maxilla and anterior mandible. At the cervical level of implant, in the anterior maxillary region, the mean of metal artefacts in percentage was 2.78 (SD: 0.15) and median was 2.75, while in the anterior mandibular region, the mean of metal artefacts in percentage was 2.85 (SD: 0.22) and median was 2.90. The difference between the median artefacts was statistically insignificant (p=0.240). Further, at the cervical and middle level of implant, in the

anterior maxillary region, the mean of metal artefacts in percentage was 2.53 (SD: 0.10) with a median of 2.50, while in the anterior mandibular region, the mean was 2.60 (SD: 0.17) and median of 2.60. The difference between the median artefacts was statistically insignificant (p=0.106). At the middle level of implant, in the anterior maxillary region, the mean of metal artefacts in percentage was 2.34 (SD: 0.09) with a median of 2.30, while in the anterior mandibular region, the mean was 2.39 (SD: 0.17) and median was 2.40. The difference between the median artefacts was statistically insignificant (p=0.302). At the middle and apical level of implant, in the anterior maxillary region, the mean of metal artefacts in percentage was 2.13 (SD: 0.11) with a median of 2.10, while in the anterior mandibular region, the mean was 2.16 (SD: 0.15) and median of 2.20. The difference between the median artefacts was statistically insignificant (p=0.348). At the apical level of implant, in the anterior maxillary region, the mean of artefacts in percentage was 1.80 (SD: 0.10) with a median of 1.80, while the anterior mandibular region, the mean was 1.79 (SD: 0.17) and median of 1.80. The difference between the median artefacts was statistically insignificant (p=0.813).

Table 3 Provides the comparison of metal artefacts in percentage between posterior maxilla and posterior mandible.

No significant difference was observed in the percentage of metal artefacts produced by implants between the posterior maxilla and posterior mandible. At the cervical level of implant, in the posterior maxillary region, the mean of metal artefacts in percentage was 2.87 (SD: 0.12) and median 2.90, while in the posterior mandibular region, the mean of metal artefacts in percentage was 2.89 (SD: 0.17) and median was 2.90. The difference between the median artefacts was statistically insignificant

(p=0.560). Further, at the cervical and middle level of implant, in the posterior maxillary region, the mean of metal artefacts in percentage was 2.65 (SD: 0.09) with a median of 2.70, while in the posterior mandibular region, the mean was 2.60 (SD: 0.12) and median of 2.60. The difference between the median artefacts was statistically insignificant (p=0.112). At the middle level of implant, in the posterior maxillary region, the mean of metal artefacts in percentage was 2.44 (SD: 0.12) with a median of 2.45, while in the posterior mandibular region, the mean was 2.40 (SD: 0.13) and median of 2.40. The difference between the median artefacts was statistically insignificant (p=0.074). At the middle and apical level of implant, in the posterior maxillary region, the mean of metal artefacts in percentage was 2.22 (SD: 0.12) with a median of 2.20, while in the posterior mandibular region, the mean was 2.19 (SD: 0.11) and median of 2.20. The difference between the median artefacts was statistically insignificant (p=0.068). At the apical level of implant, in the posterior maxillary region, the mean of metal artefacts in percentage was 1.90 (SD: 0.11) with a median of 1.90, while in the posterior mandibular region, the mean was 1.85 (SD: 0.16) and median of 1.85. The difference between the median artefacts was statistically insignificant (p=0.148).

Table 4 Provides the comparison of metal artefacts in percentage between anterior region of maxilla and mandible and posterior region of maxilla and mandible.

While comparing the metal artefacts in percentage produced by implants placed in anterior or posterior region, irrespective of jaws, the implants placed in posterior region of both maxilla and mandible showed a significantly higher percentage of artefacts at all the levels except level 1 of implant At the cervical level

of implant, in the anterior region, the mean of metal artefacts in percentage was 2.82 (SD: 0.19) and median 2.80, while in the posterior region, the mean of metal artefacts in percentage was 2.88 (SD: 0.15) and median was 2.90. The difference between the median artefacts was statistically insignificant (p=0.099). Further, at the cervical and middle level of implant, in the anterior region, the mean of metal artefacts in percentage was 2.56 (SD: 0.14) with a median of 2.50, while in the posterior region, the mean was 2.62 (SD: 0.11) and median was 2.60. The difference between the median artefacts was statistically significant (p=0.026). At the middle level of implant in the anterior region, the mean of metal artefacts in percentage was 2.37 (SD: 0.14) with a median of 2.30, while in the posterior region, the mean was 2.42 (SD: 0.13) and median was 2.40. The difference between the median artefacts was statistically significant (p=0.031). At the middle and apical level of implant, in the anterior region, the mean of artefacts in percentage was 2.14 (SD: 0.13) with a median of 2.10, while in the posterior region, the mean was 2.21 (SD: 0.12) and median of 2.20. The difference between the median artefacts was statistically significant (p=0.015). At the apical level of implant, in the anterior region, the mean of artefacts in percentage was 1.80 (SD: 0.14) with a median of 1.80, while in the posterior region, the mean was 1.88 (SD: 0.14) and median of 1.90. The difference between the median artefacts was statistically significant (p=0.012).

Table 5 Provides the comparison of metal artefacts in percentage between maxilla and mandible irrespective of anterior and posterior region.

No significant difference was observed in the in the percentage of metal artefacts produced by implants between maxilla and mandible irrespective of anatomic site. At the cervical level of implant, in the maxillary region, the mean of

metal artefacts in percentage was 2.83 (SD: 0.14) and median was 2.90, while in the mandibular region, the mean of metal artefacts in percentage was 2.87 (SD: 0.20) and median 2.90. The difference between the median artefacts was statistically insignificant (p=0.149). Further, at the cervical and middle level of implant, in the maxillary region, the mean of artefacts in percentage was 2.59 (SD: 0.12) with a median of 2.60, while in the mandibular region, the mean was 2.60 (SD: 0.15) and median of 2.60. The difference between the median artefacts was statistically insignificant (p=0.634). At the middle level of implant, in the maxillary region, the mean of artefacts in percentage was 2.39 (SD: 0.12) with a median of 2.40, while in the mandibular region, the mean was 2.39 (SD: 0.15) and median of 2.40. The difference between the median artefacts was statistically insignificant (p=0.987). At the middle and apical level of implant, in the maxillary region, the mean of artefacts in percentage was 2.17 (SD: 0.12) with a median of 2.20, while in the mandibular region, the mean was 2.18 (SD: 0.13) and median of 2.20. The difference between the median artefacts was statistically insignificant (p=0.907). At the apical level of implant, in the maxillary region, the mean of artefacts in percentage was 1.85 (SD: 0.11) with a median of 1.90, while in the mandibular region, the mean was 1.82 (SD: 0.17) and median of 1.80. The difference between the median artefacts was statistically insignificant (p=0.394).

Table 6 Provides the comparison of metal artefacts in percentage between maxilla and mandible with isolated implants.

No significant difference was observed in the percentage of metal artefacts produced by implants between maxilla and mandible with isolated implants. At the cervical level of implant, in the maxillary region, the mean of metal artefacts

percentage was 2.85 (SD: 0.14) and median 2.90, while in the mandibular region, the mean of metal artefacts was 2.90 (SD: 0.21) and median 2.90. The difference between the median artefacts was statistically insignificant (p=0.243). Further, at the cervical and middle level of implant, in the maxillary region, the mean of metal artefacts percentage was 2.61 (SD: 0.12) with a median of 2.60, while in the mandibular region, the mean was 2.59 (SD: 0.16) and median of 2.60. The difference between the median artefacts was statistically insignificant (p=0.675). At the middle level of dental implant, in the maxillary region, the mean of metal artefacts percentage was 2.40 (SD: 0.13) with a median of 2.40, while in the mandibular region, the mean was 2.40 (SD: 0.18) and median of 2.40. The difference between the median artefacts was statistically insignificant (p=0.957). At the middle and apical level of implant, in the maxillary region, the mean of metal artefacts percentage was 2.19 (SD: 0.13) with a median of 2.20, while in the mandibular region, the mean was 2.19 (SD: 0.15) and median of 2.20. The difference between the median artefacts was statistically insignificant (p=0.943). At the apical level of implant, in the maxillary region, the mean of artefacts percentage was 1.84 (SD: 0.12) with a median of 1.90, while in the mandibular region, the mean was 1.81 (SD: 0.15) and median of 1.85. The difference between the median artefacts was statistically insignificant (p=0.581).

Table 7 Provides the comparison of metal artefacts in percentage between maxilla and mandible with adjacent implants.

No significant difference was observed in the percentage of metal artefacts produced by implants between maxilla and mandible with adjacent implants.

At the cervical level of implant, in the maxillary region, the mean of metal artefacts percentage was 2.79 (SD: 0.14) and median was 2.80, while in the

mandibular region, the mean of metal artefacts was 2.85 (SD: 0.18) and median was 2.90. The difference between the median artefacts was statistically insignificant (p=0.167). Further, at the cervical and middle level of implant, in the maxillary region, the mean of metal artefacts percentage was 2.56 (SD: 0.11) with a median of 2.50, while in the mandibular region, the mean was 2.61 (SD: 0.14) and median of 2.60. The difference between the median artefacts was statistically insignificant (p=0.162). At the middle level of implant, in the maxillary region, the mean of metal artefacts percentage was 2.37 (SD: 0.10) with a median of 2.30, while in the mandibular region, the mean was 2.39 (SD: 0.13) and median of 2.40. The difference between the median artefacts was statistically insignificant (p=0.550). At the middle and apical level of implant, in the maxillary region, the mean of metal artefacts percentage was 2.16 (SD: 0.11) with a median of 2.20, while in the mandibular region, the mean was 2.17 (SD: 0.12) and median of 2.20. The difference between the median artefacts was statistically insignificant (p=0.848). At the apical level of implant, in the maxillary region, the mean of artefacts percentage was 1.86 (SD: 0.10) with a median of 1.90, while in the mandibular region, the mean was 1.83 (SD: 0.18) and median of 1.80. The difference between the median artefacts was statistically insignificant (p=0.500).

Table 8 Provides the comparison of metal artefacts in percentage between isolated and adjacent implants.

No statistically significant difference was observed in the percentage of metal artefacts produced by implants between isolated and adjacent implants.

At the cervical level of isolated implants, the mean of metal artefacts percentage was 2.87 (SD: 0.18) and median 2.90, while for adjacent implants, the

mean of metal artefacts percentage was 2.82 (SD: 0.16) and median 2.80. The difference between the median artefacts was statistically insignificant (p=0.107). Further, at the cervical and middle level of isolated implants, the mean of artefacts percentage was 2.60 (SD: 0.14) with a median of 2.60, while for adjacent implants, the mean was 2.59 (SD: 0.13) and median of 2.60. The difference between the median artefacts was statistically insignificant (p=0.641). At the middle level of isolated implants, the mean of artefacts percentage was 2.40 (SD: 0.15) with a median of 2.40, while for adjacent implants, the mean was 2.38 (SD: 0.12) and median of 2.40. The difference between the median artefacts was statistically insignificant (p=0.309). At the middle and apical level of isolated implants, the mean of artefacts percentage was 2.19 (SD: 0.14) with a median of 2.20, while for adjacent implants, the mean was 2.16 (SD: 0.12) and median of 2.20. The difference between the median artefacts was statistically insignificant (p=0.313). At the apical level of isolated implants, the mean of artefacts percentage was 1.83 (SD: 0.14) with a median of 1.90, while for adjacent implant, the mean was 1.85 (SD: 0.15) and median of 1.85. The difference between the median artefacts was statistically insignificant (p=0.645).

Table 9 Provides the comparison of metal artefacts in percentage produced across 5 different levels of dental implants.

A statistically significant difference was observed in the percentage of metal artefacts produced by implants across 5 different levels of dental implants.

The mean of artefactspercentage at cervical level of implant was 2.85 (SD: 0.17) with a median of 2.90, at cervical and middle level of implant was 2.59 (SD: 0.13) with a median of 2.60, at middle level of dental implant was 2.39 (SD: 0.14) with a median of 2.40, at middle and apical level of implant was 2.18 (SD: 0.13) with

a median of 2.20 and at apical level of implant was 1.84 (SD: 0.14) with a median of 1.90. The difference in the median of artefacts was statistically significant across slices ($p < 0.0001$). The pair wise analysis using Mann-Whitney test resulted into significant difference between all the paired comparisons.

Table 10 Provides descriptive statistics for metal artefacts in percentage across different anatomical sites and across 5 different levels of dental implants.

There were 26 implants in the anterior maxillary region. The mean of metal artefacts in percentage at the cervical level of dental implant was 2.78 (SD: 0.15), at the cervical and middle level of implant was 2.53 (SD: 0.10), the middle level of implant was 2.34 (SD: 0.09), the middle and apical level of implant was 2.13 (SD: 0.11) and the apical level of implant was 1.80 (SD: 0.10).In the posterior maxillary region, the mean of metal artefacts in percentage at the cervical level of implant was 2.87 (SD: 0.12), at the cervical and middle level of implant was 2.65 (SD: 0.09), the middle level of implant was 2.44 (SD: 0.12), the middle and apical level of implant was 2.22 (SD: 0.12) and the apical level of implant was 1.90 (SD: 0.11).In the anterior mandibular region, the mean of metal artefacts in percentage at the cervical level of implant was 2.85 (SD: 0.22), at the cervical and middle level of implant was 2.60 (SD: 0.17), the middle level of implant was 2.39 (SD: 0.17), the middle and apical level of implant was 2.16 (SD: 0.15) and the apical level of implant was 1.79 (SD: 0.17). In the posterior mandibular region, the mean of metal artefacts in percentage at the cervical level of implant was 2.89 (SD: 0.17), at the cervical and middle level of implant was 2.60 (SD: 0.12), the middle level of implant was 2.40 (SD: 0.13), the middle and apical level of implant was 2.19 (SD: 0.11) and the apical level of implant was 1.85 (SD: 0.16).

DISCUSSION

CBCT is extensively used in dental implantology for the pre and post operative evaluation of dental implant and its surrounding anatomical structure[5,59]. In the pre-operative phase, it is used to evaluate the quality and quantity of alveolar bone before implant placement, while in post-operative phase, it is used to assess the signs and symptoms of peri-implantitis and to evaluate marginal bone level as well as bone implant contact[7]. However, in post-operative cases, the presence of already placed implants produces artefacts of metal in the CBCT images.

Metal artefacts are one of the most challenging problem faced in the readings of CBCT images[8]. These artefacts are structures visualised in the image which do not actually exist[9]. They decrease the quality of images and has deleterious effect on the interpretation and diagnosis of the CBCT scan[10,11]. Artefacts in CBCT are affected by various factors such as the material of implant, large FOVs, CBCT machine, low kVp, anatomic site and small voxel size.[8]

In CBCT, the images are made up of voxels. Each voxel is recognized by a gray values which reflects the degree of attenuation of X rays, while passing through the study objects. In the CBCT images, the gray values are influenced by atomic number and density of the object[2,3]. Dental implants are made up of different metals such as titanium, zirconium, and titanium-zirconium alloy. They have high density and atomic number as compared to that of bone and soft tissue elements[1]. Hence, they lead to formation of beam hardening artefacts due to variations in the attenuation and absorption of beam of X ray[12, 13]. While passing through the dental implants, low energy photons are absorbed instead of high energy photons[12, 14, 16]. Thus, these artefacts appear like hyper dense streaks radiating from high density object, when hypo dense area is interspersed between them**[12, 14, 15]**.

It has been observed in various studies [23,24,25,26,27,28] that Zirconium implants produces the most metal artefacts and titanium produce the least metal due to less atomic number and density. This study aimed to quantify metal artefacts produced in the CBCT scans and since titanium implants are most commonly used in clinical practice in this part of world and also to avoid bias all the scans used were of titanium implants.

In the present study, while comparing the metal artefacts produced by implants placed in anterior or posterior region, irrespective of jaws, the implants placed in posterior region of both maxilla and mandible showed a significantly higher percentage of artefacts at all the levels except level 1 of implant (Table 4). **Oliviera *et al.*[3]** in their study assessed the impact of anatomic site on the grey values of CBCT scans and found that gray values of the similar object differed according to their anatomical location. In contrast to the present study, **Machado *et al.*[2]** observed a

greater number of artefacts in the implants placed in the anterior region of jaws and only at apical and middle level of implant. This difference could be due to the fact that in their study most of the scans had more than one adjacent implants. **Valizadeh *et al.*[18]** in their study observed that position of object within FOV affects the gray values in the CBCT images via interaction of X rays and surrounding anatomic structures. Similarly, the effect of the exomass, i.e. the entire craniofacial area located inside and outside the FOV explains the variation in artefacts as per anatomical site. Thus, adjacent anatomical structures, such as the presence of skull and spinal column, affects the gray value measurements in the maxilla and mandible[5,23].

No significant difference was observed in the percentage of metal artefacts produced by dental implants between maxilla and mandible irrespective of anatomic site (Table 5). However, in contrast to the present study, **Machado *et al.*[2]** reported a greater percentage of artefacts in the implants placed in the mandibular region of jaw at the apical and middle level of implant. Literature suggests that the thickness and density of bone of maxilla and mandible will affect the grey values[2].

This study has quantified the artefacts at 5 different levels of implant and could get significant difference in the gray values among the selected 5 levels as shown in Table 9 whereas study by **Machado *et al.*[2]** could not get significant difference at 3 levels i.e cervical, middle and apical. And the probable reason for this could be due to presence of prosthesis placed over the implants. As prosthetic crowns such as cobalt, chromium have higher atomic number [16] as compared to that of titanium, more artefacts were formed at the cervical level of implant. Similar findings were observed by **Machado *et al.*[2]** who reported more numbers of formation of

artifact at the cervical level of implant when measurements were carried out at three different levels of implants i.e. Apical, middle, cervical.

It is known that implant being a high density metal attenuates more X ray beam as compared to that of soft tissues and bone[1]. Therefore, it was predicted that the greater percentage of artefacts would be obtained between the 2 adjacent implants as compared to single or isolated implant **Luckow *et al.*[38]** in their study observed that greater amount of artefact formation can be observed at a particular position when the the X-rays transverses along the axis of the maxillary or mandibular jaw and thus interacts with teeth, adjoining bone and dental implants, on single plane. However, in the present study non significant difference was observed in the percentage of artefacts produced around adjacent or isolated implants as shown in Table 8. Similar results were found by **Machado *et al.*[2]** as they also did not obtain greater percentage of artifact quantification produced by adjacent dental implant. The probable reason of this finding would be attributed to the use of small ROI (10x10 mm). Therefore, use of wider ROI would have produced greater artifact quantification between the adjacent dental implant.

Rabelo *et al.*[50] in their study measured artefacts formation by various root canal filling materials in the CBCT images using variables like mA and kVp. They observed that exposure parameters like kVp and mA had no significant association with artefact formation. The author also mentioned that there can be other factors influencing the artefacts like; voxel size, slice thickness and FOV dimensions. In the present study, the above mentioned factors were not considered while calculating the artifact quantification but used gray values with respect to the anatomical location. Future in vitro studies can be designed to evaluate the effect of other parameters on

artefacts generation by implants or other similar material. This research will aid in diagnostic accuracy and would help to improve dental practice with better scans or minimum artefacts.

From the above results, it can be concluded that artefacts are always produced by metals and are visible in the images of CBCT. Also, the anatomic location influences the amount of metal artefacts generated, as we found more predilection for the posterior region of maxilla and mandible.

SUMMARY AND CONCLUSION

The present retrospective and observational study was carried out to assess the effect of anatomic location on artefact formation produced by titanium dental implant in CBCT. Total 104 CBCT scans containing titanium dental implants were obtained from private CBCT Centre and were equally divided into 4 groups according to the location of the implant.

Group I —Included 26 Implants placed in anterior maxilla;

Group II —Included 26 Implants placed in posterior maxilla;

Group III —Included 26 Implants placed in anterior mandible;

Group IV —Included 26 Implants placed in posterior mandible.

The implants were further classified into isolated and adjacent implant.

All the CBCT scans was evaluated at 5 different axial levels:

1. At cervical level
2. Between cervical and middle level
3. Middle level
4. Between middle and apical level
5. Apical level

Image J Software was used for quantifying the percentage of metal artefacts for the evaluation of axial sections for each implant. The data generated was analyzed statistically and the results of the study were tabulated.

The results of present study indicated that

1. No significant difference was observed in the percentage of metal artefacts produced by implants between the anterior maxilla and anterior mandible.

2. No significant difference was observed in the percentage of metal artefacts produced by implants between the posterior maxilla and posterior mandible.

3. A statistically significant difference was observed in the percentage of metal artefacts produced by implants placed in posterior region of maxilla and mandible at all the levels of implant except level 1.

4. No significant difference was observed in the in the percentage of metal artefacts produced by implants between maxilla and mandible irrespective of anatomic site.

5. No significant difference was observed in the percentage of metal artefacts produced by implants between maxilla and mandible with isolated implants..

6. No significant difference was observed in the percentage of metal artefacts produced by implants between maxilla and mandible with adjacent implants.

7. No statistically significant difference was observed in the percentage of metal artefacts produced by implants between isolated and adjacent implants.

8. A statistically significant difference was observed in the percentage of metal artefacts produced by implants across 5 different levels of dental implants.

Therefore, this study concludes that the artefact formation is influenced by the anatomic location, where we found predilection for posterior region of both the jaws. Also, the quantification of metal artefacts at equidistant axial section from cervical to apical region of implant showed significant intergroup comparison with higher percentage of quantification at the cervical level.

Limitation and future prospective

1. The sample size of the present study was limited to 104 CBCT Scans. Therefore, large sample size would be desirable to substantiate the present study results.

2. The study has not considered factors such as FOV, voxel size and slice thickness for artefact generation by implants or other similar material. Hence, future in vitro studies can be designed to evaluate the effect of these parameters.

REFERENCES

1. Cremonini CC, Dumas M, Pannuti CM, Neto JB, Cavalcanti MG, Lima LA. Assessment of linear measurements of bone for implant sites in the presence of metallic artefacts using cone beam computed tomography and multislice computed tomography. International journal of oral and maxillofacial surgery. 2011; 40(8):845-850.

2. Machado AH, Fardim KA, de Souza CF, Sotto-Maior BS, Assis NM, Devito KL. Effect of anatomical region on the formation of metal artefacts produced by dental implants in cone beam computed tomographic images. Dentomaxillofacial Radiology. 2018 Jan; 47(1):1-6.

3. Oliveira ML, Tosoni GM, Lindsey DH, Mendoza K, Tetradis S, Mallya SM. Influence of anatomical location on CT numbers in cone beam computed

tomography. Oral surgery, oral medicine, oral pathology and oral radiology. 2013; 115(4):558-564.

4. White SC, Pharoah MJ. Oral Radiology:Principles and interpretation1st South Asia edition, Elsevier Health Sciences,. pp : 185-198.

5. Smeets R, Schöllchen M, Gauer T, Aarabi G, Assaf AT, Rendenbach C, Beck-Broichsitter B, Semmusch J, Sedlacik J, Heiland M, Fiehler J. Artefacts in multimodal imaging of titanium, zirconium and binary titanium–zirconium alloy dental implants: an in vitro study. Dentomaxillofacial Radiology. 2017; 46(2):1-9.

6. Min CK, Kim KA. Reducing metal artefacts between implants in cone-beam CT by adjusting angular position of the subject. Oral Radiology. 2021; 37(3):385-394.

7. Bornstein MM, Horner K, Jacobs R. Use of cone beam computed tomography in implant dentistry: current concepts, indications and limitations for clinical practice and research. Periodontology 2000. 2017;73(1):51-72.

8. Terrabuio BR, Carvalho CG, Peralta-Mamani M, da Silva Santos PS, Rubira-Bullen IR, Rubira CM. Cone-beam computed tomography artefacts in the presence of dental implants and associated factors: an integrative review. Imaging Science in Dentistry. 2021 Jun;51(2):93-106.

9. Schulze RK, Berndt D, d'Hoedt B. On cone-beam computed tomography artefacts induced by titanium implants. Clinical oral implants research. 2010; 21(1):100-107.

10. Veikutis V, Budrys T, Basevicius A, Lukosevicius S, Gleizniene R, Unikas R, Skaudickas D. Artefacts in computer tomography imaging: how it can really affect diagnostic image quality and confuse clinical diagnosis? Journal of Vibroengineering. 2015 ;17(2):995-1002.

11. Malav Thakrar D, Solanki A, Bhargava S, Asthana G, Parmar G. Artefacts-The Black Spot of CBCT. Journal of Government Dental College and Hospital. 2016; 2(2):5-10.

12. Schulze R, Heil U, Gross D, Bruellmann DD, Dranischnikow E, Schwanecke U, Schoemer E. Artefacts in CBCT: a review. Dentomaxillofacial Radiology. 2011;40(5):265-273.

13. Vasconcelos TV, Bechara BB, McMahan CA, Freitas DQ, Noujeim M. Evaluation of artefacts generated by zirconium implants in cone-beam computed tomography images. Oral surgery, oral medicine, oral pathology and oral radiology.2017;123 (2):265-272.

14. Pauwels R, Stamatakis H, Bosmans H, Bogaerts R. Quantification of metal artefacts on cone beam computed tomography images. Clinical oral implants research.2011; 24:94-99.

15. Jaju PP, Jain M, Singh A, Gupta A. Artefacts in cone beam CT. Open Journal of Stomatology. 2013; 3(5):292-297.

16. Chindasombatjaroen J, Kakimoto N, Murakami S, Maeda Y, Furukawa S. Quantitative analysis of metallic artefacts caused by dental metals: comparison

of cone-beam and multi-detector row CT scanners. Oral Radiology.2011; 27(2):114-120.

17. Benic GI, Sancho-Puchades M, Jung RE, Deyhle H, Hämmerle CH. In vitro assessment of artefacts induced by titanium dental implants in cone beam computed tomography. Clinical Oral implants research. 2013; 24(4):378-383.

18. Valizadeh S, Vasegh Z, Rezapanah S, Safi Y, Khaeazifard MJ. Effect of object position in cone beam computed tomography field of view for detection of root fractures in teeth with intracanal posts. Iran J Radiol 2015; 12(4): 1-8.

19. Venkatesh E, Elluru SV. Cone beam computed tomography: basics and applications in dentistry. Journal of Istanbul University faculty of Dentistry. 2017;51:S102 -S121.

20. Jaju PP, Jaju SP. Cone-beam computed tomography: Time to move from ALARA to ALADA. Imaging science in dentistry. 2015 Dec 1;45(4):263-265.

21. Nagarajappa AK, Dwivedi N, Tiwari R. Artefacts: The downturn of CBCT image. Journal of International Society of Preventive & Community Dentistry.2015 ;5(6):440-445.

22. Vahdani N, Moudi E, Ghobadi F, Mohammadi E, Bijani A, Haghanifar S. Evaluation of the Metal Artifact Caused by Dental Implants in Cone Beam Computed Tomography Images. Maedica. 2020; 15(2):224-229.

23. Sancho-Puchades M, Hämmerle CH, Benic GI. In vitro assessment of artefacts induced by titanium, titanium–zirconium and zirconium dioxide implants in

cone-beam computed tomography. Clinical oral implants research.2015; 26(10):1222-1228.

24. Kocasarac HD, Ustaoglu G, Bayrak S, Katkar R, Geha H, Deahl II ST, Mealey BL, Danaci M, Noujeim M. Evaluation of artefacts generated by titanium, zirconium, and titanium–zirconium alloy dental implants on MRI, CT, and CBCT images: A phantom study. Oral surgery, oral medicine, oral pathology and oral radiology. 2019;127 (6):535-544.

25. Fontenele RC, Nascimento EH, Vasconcelos TV, Noujeim M, Freitas DQ. Magnitude of cone beam CT image artefacts related to zirconium and titanium implants: impact on image quality. Dentomaxillofacial Radiology. 2018; 47(6): 1-7.

26. Bashizadeh Fakhar H, Sharifian H, Niknami M, Iranmanesh M. Artefacts of Titanium, Zirconium, and Binary Titanium-Zirconium Abutments in Compute Tomography, Cone Beam Computed Tomography, and Magnetic Resonance Imaging. Journal of Dental Materials and Techniques. 2020;9(1):10-14.

27. Kocasarac HD, Freitas D, Ustaoglu G , Oliveira M, Koenig L. Assessment of CBCT image artefacts generated by implants located in the exomass. Oral surgery, oral medicine, oral pathology and oral radiology. 2020;130(2):e60.

28. Demirturk Kocasarac H, Koenig LJ, Ustaoglu G, Oliveira ML, Freitas DQ. CBCT image artefacts generated by implants located inside the field of view or in the exomass. Dentomaxillofacial Radiology. 2021;51(2):20210092.

29. Martins LA, Queiroz PM, Nejaim Y, Vasconcelos KD, Groppo FC, Haiter-Neto F. Evaluation of metal artefacts for two CBCT devices with a new dental arch phantom. Dentomaxillofacial Radiology. 2020; 49(5):1-8.

30. Razavi T, Palmer RM, Davies J, Wilson R, Palmer PJ. Accuracy of measuring the cortical bone thickness adjacent to dental implants using cone beam computed tomography. Clin Oral Implants Res 2010; 21: 718-725.

31. Shokri A, Jamalpour MR, Khavid A, Mohseni Z, Sadeghi M. Effect of exposure parameters of cone beam computed tomography on metal artifact reduction around the dental implants in various bone densities. BMC medical imaging. 2019; 19(1):1-10.

32. Junqueira LC, Carneiro J. Histologia básica. 10th ed. Rio de Janeiro: Guanabara Koogan S.A.; 2004.

33. Szabó BT, Dobai A, Dobo-Nagy C. Cone-Beam Computed Tomography in Dentomaxillofacial Radiology. In Novel Imaging and Spectroscopy 2020:127-146.

34. Syam S, Maheswari TU. Artefacts in Cone Beam Computed Tomography–A Retrospective study. Journal of Pharmaceutical Sciences and Research. 2019; 11(5):1914-1917.

35. Bhoosreddy AR, Sakhavalkar PU. Image deteriorating factors in cone beam computed tomography, their classification, and measures to reduce them: A pictorial essay. Journal of Indian Academy of Oral Medicine and Radiology. 2014; 26(3):293-297.

36. Sinha A, Mishra A, Srivastava S, Sinha PM, Chaurasia A. Understanding artefacts in cone beam computed tomography. International Journal of Maxillofacial Imaging. 2016; 2(2):51-54.

37. Makins SR. Artefacts interfering with interpretation of cone beam computed tomography images. Dental Clinics of North America. 2014; 58(3):485-495.

38. Luckow M, Deyhle H, Beckmann F, Dagassan-Berndt D, Müller B. Tilting the jaw to improve the image quality or to reduce the dose in cone-beam computed tomography. European journal of radiology. 2011; 80(3):e389-393.

39. Bechara BB, Moore WS, McMahan CA, Noujeim M. Metal artifact reduction with cone beam CT: an in vitro study. Dentomaxillofacial Radiology. 2012; 41(3):248-253.

40. Bechara B, McMahan CA, Geha H, Noujeim M. Evaluation of a cone beam CT artifact reduction algorithm. Dentomaxillofacial Radiology. 2012; 41(5):422-428

41. Esmaeili F, Johari M, Haddadi P, Vatankhah M. Beam hardening artefacts: comparison between two cone beam computed tomography scanners. Journal of dental research, dental clinics, dental prospects. 2012;6(2):49-53.

42. Parsa A, Ibrahim N, Hassan B, Motroni A, Van der Stelt P, Wismeijer D. Influence of cone beam CT scanning parameters on grey value measurements at an implant site. Dentomaxillofacial Radiology. 2013; 42(3):1-7.

43. Naitoh M, Saburi K, Gotoh K, Kurita K, Ariji E. Metal artefacts from posterior mandibular implants as seen in CBCT. Implant Dent 2013; 22(2): 151-154.

44. Parsa A, Ibrahim N, Hassan B, Syriopoulos K, Van Der Stelt P. Assessment of metal artifact reduction around dental titanium implants in cone beam CT. Dentomaxillofacial Radiology. 2014; 43(7):1-6.

45. Oliveira ML, Freitas DQ, Ambrosano GM, Haiter-Neto F. Influence of exposure factors on the variability of CBCT voxel values: a phantom study. Dentomaxillofacial Radiology. 2014;43(6):1-6.

46. Panjnoush M, Kheirandish Y, Kashani PM, Fakhar HB, Younesi F, Mallahi M. Effect of exposure parameters on metal artefacts in cone beam computed tomography. Journal of Dentistry (Tehran, Iran). 2016; 13(3):143-150.

47. Bashizadeh Fakhar H, Sharifian H, Niknami M, Iranmanesh M. Artefacts of Titanium, Zirconium, and Binary Titanium-Zirconium Abutments in Computed Tomography, Cone Beam Computed Tomography, and Magnetic Resonance Imaging. Journal of Dental Materials and Techniques. 2020;9(1):10-14.

48. Queiroz PM, Santaella GM, da Paz TD, Freitas DQ. Evaluation of a metal artifact reduction tool on different positions of a metal object in the FOV. Dentomaxillofacial Radiology. 2017; 46(3):1-4.

49. Codari M, de Faria Vasconcelos K, Ferreira Pinheiro Nicolielo L, Haiter Neto F, Jacobs R. Quantitative evaluation of metal artefacts using different CBCT

devices, high-density materials and field of views. Clinical oral implants research.2017 ;28(12):1509-1514.

50. Rabelo KA, Cavalcanti YW, de Oliveira Pinto MG, Sousa Melo SL, Campos PSF, de Andrade Freitas Oliveira LS, et al. Quantitative assessment of image artefacts from root filling materials on CBCT scans made using several exposure parameters. Imaging Sci Dent 2017; 47: 189–97.

51. Sheridan RA, Chiang YC, Decker AM, Sutthiboonyapan P, Chan HL, Wang HL. The effect of implant-induced artefacts on interpreting adjacent bone structures on cone-beam computed tomography scans. Implant Dentistry. 2017;26(6):1-5.

52. Freitas DQ, Fontenele RC, Nascimento EH, Vasconcelos TV, Noujeim M. Influence of acquisition parameters on the magnitude of cone beam computed tomography artefacts. Dentomaxillofacial Radiology. 2018; 47(8):1-11.

53. Akay G, Karatas MS, Karadag O, Ucok O, Gungor K. The incidence of artefacts in cone beam computed tomography images: A pilot study. Annals of Medical Research. 2019; 26(11):2581-2586.

54. Safi Y, Fazlyab M, Asgary S, Fazlalipour S. A Novel Technique for Minimizing the Metal Artefacts on Anterior Teeth in Cone-Beam Computed Tomography. Iranian Endodontic Journal. 2019; 14(1):79-83.

55. Fontenele RC, Nascimento EH, Santaella GM, Freitas DQ. Does the metal artifact reduction algorithm activation mode influence the magnitude of artefacts in CBCT images?. Imaging science in dentistry. 2020;50(1):23-30.

56. Kim YH, Lee C, Han SS, Jeon KJ, Choi YJ, Lee A. Quantitative analysis of metal artifact reduction using the auto-edge counting method in cone-beam computed tomography. Scientific Reports. 2020;10(1):1-6.

57 Shahmirzadi S, Sharaf RA, Saadat S, Moore WS, Geha H, Tamimi D, Kocasarac HD. Assessment of the efficiency of a pre-versus post-acquisition metal artifact reduction algorithm in the presence of 3 different dental implant materials using multiple CBCT settings: An in vitro study. Imaging Science in Dentistry. 2021;51(1):1-7.

58. Salemi F, Jamalpour MR, Eskandarloo A, Tapak L, Rahimi N. Efficacy of metal artifact reduction algorithm of cone-beam computed tomography for detection of fenestration and dehiscence around dental implants. Journal of Biomedical Physics & Engineering. 2021;11(3): 1-10.

59 Mukherji A, Singh MP, Nahar P, Goel S, Mathur H, Khan Z. Why CBCT is imperative for implant placement. Journal of Indian Academy of Oral Medicine and Radiology. 2019 ;31(4):363-369.

TABLE AND GRAPHS

Table 1: Distribution of dental implants in study groups

		Proximity of implants					
		Isolated		Adjacent		Total	
		n	%	n	%	N	%
Site	Anterior maxilla	15	27.8%	11	22.0%	26	25.0%
	Posterior maxilla	15	27.8%	11	22.0%	26	25.0%
	Anterior mandible	11	20.4%	15	30.0%	26	25.0%
	Posterior mandible	13	24.1%	13	26.0%	26	25.0%

Table 2: Comparison of metal artefacts in percentage between anterior maxilla and anterior mandible.

5 different levels of Dental implant			Cervical level	Cervical and middle level	Middle Level	Middle and apical level	Apical level
Site	Maxillary	N	26	26	26	26	26
		Mean	2.78	2.53	2.34	2.13	1.80
		SD	0.15	0.10	0.09	0.11	0.10
		Median	2.75	2.50	2.30	2.10	1.80
	Mandibular	N	26	26	26	26	26
		Mean	2.85	2.60	2.39	2.16	1.79
		SD	0.22	0.17	0.17	0.15	0.17
		Median	2.90	2.60	2.40	2.20	1.80
P-value*			0.240	0.106	0.302	0.348	0.813

SD: Standard deviation; *Obtained using Mann-Whitney U test

Table 3: Comparison of metal artefacts in percentage between posterior maxilla and posterior mandible.

5 different levels of dental implant			Cervical level	Cervical and middle level	Middle level	Middle and apical	Apical level
Site	Maxillary	N	26	26	26	26	26
		Mean	2.87	2.65	2.44	2.22	1.90
		SD	0.12	0.09	0.12	0.12	0.11
		Median	2.90	2.70	2.45	2.20	1.90
	Mandibular	N	26	26	26	26	26
		Mean	2.89	2.60	2.40	2.19	1.85
		SD	0.17	0.12	0.13	0.11	0.16
		Median	2.90	2.60	2.40	2.20	1.85
P-value*			0.560	0.112	0.074	0.068	0.148

SD: Standard deviation; *Obtained using Mann-Whitney U test

Table 4: Comparison of metal artefacts in percentage between anterior region of maxilla and mandible and posterior region of maxilla and mandible.

5 different levels of dental implant			Cervical level	Cervical and middle level	Middle Level	Middle and apical	Apical level
Site	Anterior region of both jaws	N	52	52	52	52	52
		Mean	2.82	2.56	2.37	2.14	1.80
		SD	0.19	0.14	0.14	0.13	0.14
		Median	2.80	2.50	2.30	2.10	1.80
	Posterior region of both jaws	N	52	52	52	52	52
		Mean	2.88	2.62	2.42	2.21	1.88
		SD	0.15	0.11	0.13	0.12	0.14
		Median	2.90	2.60	2.40	2.20	1.90
P-value*			0.099	**0.026**	**0.031**	**0.015**	**0.012**

SD: Standard deviation; *Obtained using Mann-Whitney U test; Bold p-values indicate statistical significance.

Table 5 Comparison of metal artefacts in percentage between maxilla and mandible irrespective of anterior and posterior region.

5 different levels of dental implant			Cervical level	Cervical and middle level	Middle level	Middle and apical level	Apical level
Site	Maxillary	N	52	52	52	52	52
		Mean	2.83	2.59	2.39	2.17	1.85
		SD	0.14	0.12	0.12	0.12	0.11
		Median	2.90	2.60	2.40	2.20	1.90
	Mandible	N	52	52	52	52	52
		Mean	2.87	2.60	2.39	2.18	1.82
		SD	0.20	0.15	0.15	0.13	0.17
		Median	2.90	2.60	2.40	2.20	1.80
P-value*			0.149	0.634	0.987	0.907	0.394

SD: Standard deviation; *Obtained using Mann-Whitney U test

Table 6: Comparison of metal artefacts in percentage between maxilla and mandible with isolated implants.

5 different levels of dental implant			Cervical Level	Cervical and middle level	Middle level	Middle and apical level	Apical level
Region	Maxillary	N	30	30	30	30	30
		Mean	2.85	2.61	2.40	2.19	1.84
		SD	0.14	0.12	0.13	0.13	0.12
		Median	2.90	2.60	2.40	2.20	1.90
	Mandible	N	24	24	24	24	24
		Mean	2.90	2.59	2.40	2.19	1.81
		SD	0.21	0.16	0.18	0.15	0.15
		Median	2.90	2.60	2.40	2.20	1.85
P-value*			0.243	0.675	0.957	0.943	0.581

SD: Standard deviation; *Obtained using Mann-Whitney U test

Table 7: Comparison of metal artefacts in percentage between maxilla and mandible with adjacent implants

5 different levels of dental implant			Cervical level	Cervical and middle level	Middle level	Middle and apical level	Apical level
Site	Maxillary	N	22	22	22	22	22
		Mean	2.79	2.56	2.37	2.16	1.86
		SD	0.14	0.11	0.10	0.11	0.10
		Median	2.80	2.50	2.30	2.20	1.90
	Mandibular	N	28	28	28	28	28
		Mean	2.85	2.61	2.39	2.17	1.83
		SD	0.18	0.14	0.13	0.12	0.18
		Median	2.90	2.60	2.40	2.20	1.80
P-value*			0.167	0.162	0.550	0.848	0.500

SD: Standard deviation; *Obtained using Mann-Whitney U test

Table 8: Comparison of metal artefacts in percentage caused by isolated and adjacent implants irrespective of maxilla and mandible.

5 different levels of dental implant			Cervical level	Cervical and middle level	Middle Level	Middle and apical level	Apical Level
Implants	Isolated	N	54	54	54	54	54
		Mean	2.87	2.60	2.40	2.19	1.83
		SD	0.18	0.14	0.15	0.14	0.14
		Median	2.90	2.60	2.40	2.20	1.90
	Adjacent	N	50	50	50	50	50
		Mean	2.82	2.59	2.38	2.16	1.85
		SD	0.16	0.13	0.12	0.12	0.15
		Median	2.80	2.60	2.40	2.20	1.85
P-value*			0.107	0.641	0.309	0.313	0.645

SD: Standard deviation; *Obtained using Mann-Whitney U test

Table 9: Comparison of metal artefacts in percentage produced across 5 different levels of dental implants.

		5 different levels of dental implant				
		Cervical level	Cervical and middle level	Middle level	Middle and apical level	Apical level
Artifacts	N	104	104	104	104	104
	Mean	2.85	2.59	2.39	2.18	1.84
	SD	0.17	0.13	0.14	0.13	0.14
	Median	2.90^{a}	2.60^{b}	2.40^{c}	2.20^{d}	1.90^{e}
P-value*		< **0.0001**				

*Obtained using Kruskal-Wallis test; SD: Standard deviation; Bold p-value indicate statistical significance; Different alphabets in the superscript indicate significant difference in the pairwise comparison.

Table 10) Descriptive statistics for metal artefacts in percentage across different anatomical sites and across 5 different levels of dental implants.

5 different levels of dental implant			Cervical level	Cervical and middle level	Middle level	Middle and apical level	Apical level
Maxillary	Anterior	N	26	26	26	26	26
		Mean	2.78	2.53	2.34	2.13	1.80
		SD	0.15	0.10	0.09	0.11	0.10
		Median	2.75	2.50	2.30	2.10	1.80
	Posterior	N	26	26	26	26	26
		Mean	2.87	2.65	2.44	2.22	1.90
		SD	0.12	0.09	0.12	0.12	0.11
		Median	2.90	2.70	2.45	2.20	1.90
Mandible	Anterior	N	26	26	26	26	26
		Mean	2.85	2.60	2.39	2.16	1.79
		SD	0.22	0.17	0.17	0.15	0.17
		Median	2.90	2.60	2.40	2.20	1.80
	Posterior	N	26	26	26	26	26
		Mean	2.89	2.60	2.40	2.19	1.85
		SD	0.17	0.12	0.13	0.11	0.16
		Median	2.90	2.60	2.40	2.20	1.85

GRAPHS

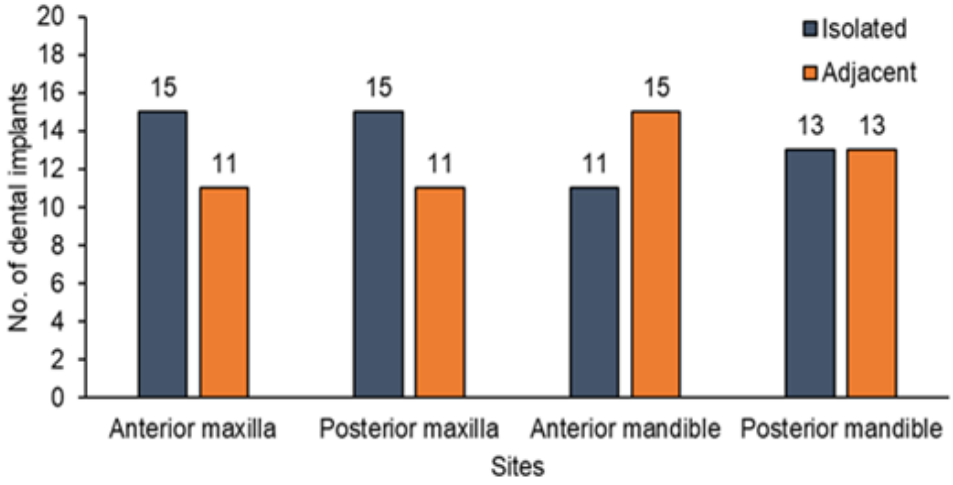

Figure 1: Double bar chart showing number of dental implants according to the anatomical sites and proximity of implant.

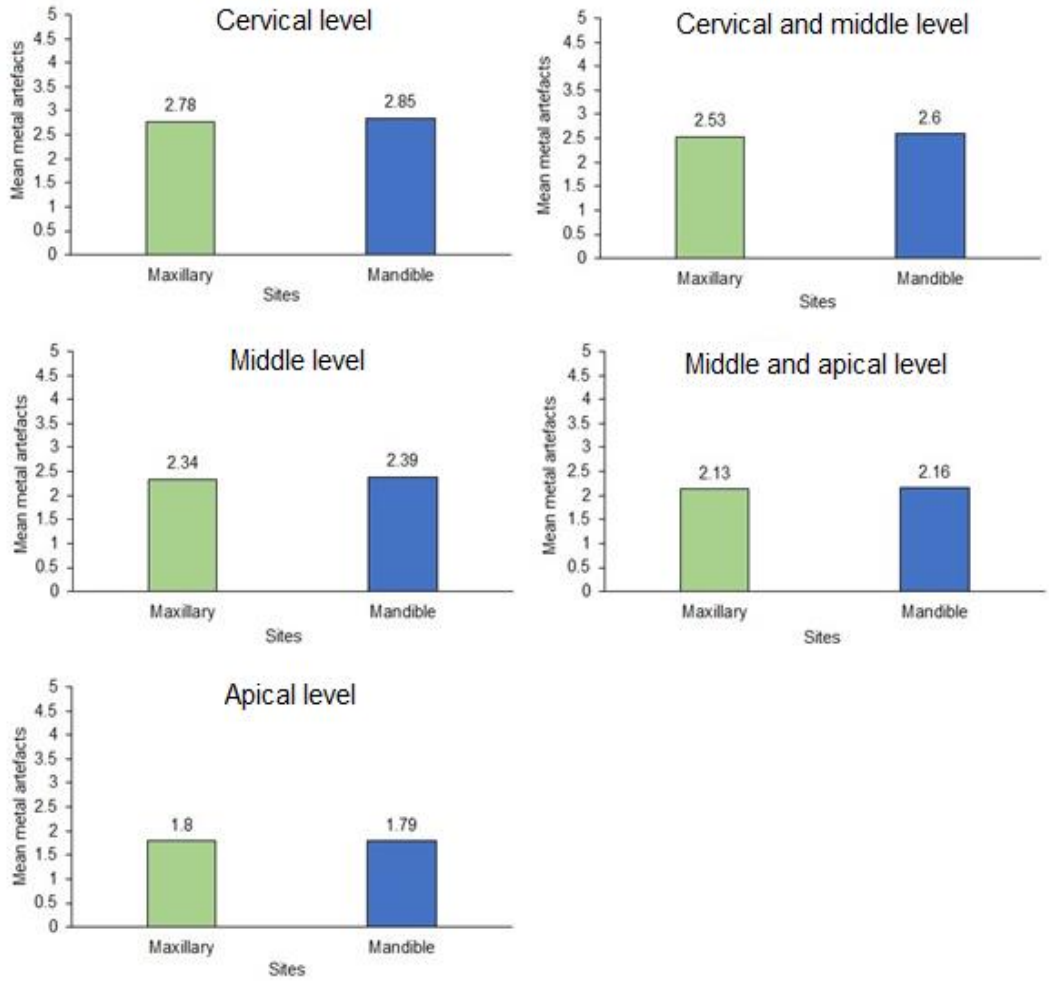

Figure 2: Column charts showing mean of metal artefacts in percentage in anterior maxilla and anterior mandible.

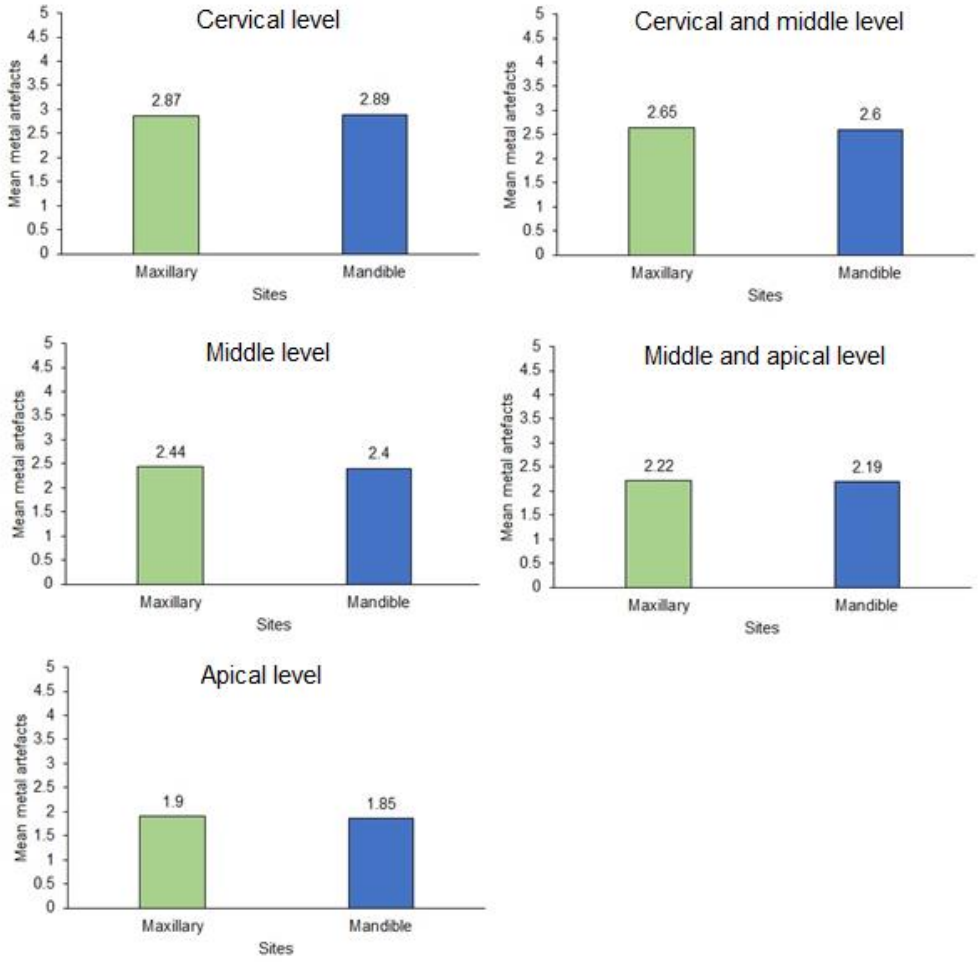

Figure 3: Column charts showing mean of metal artefacts in percentage in posterior maxilla and posterior mandible.

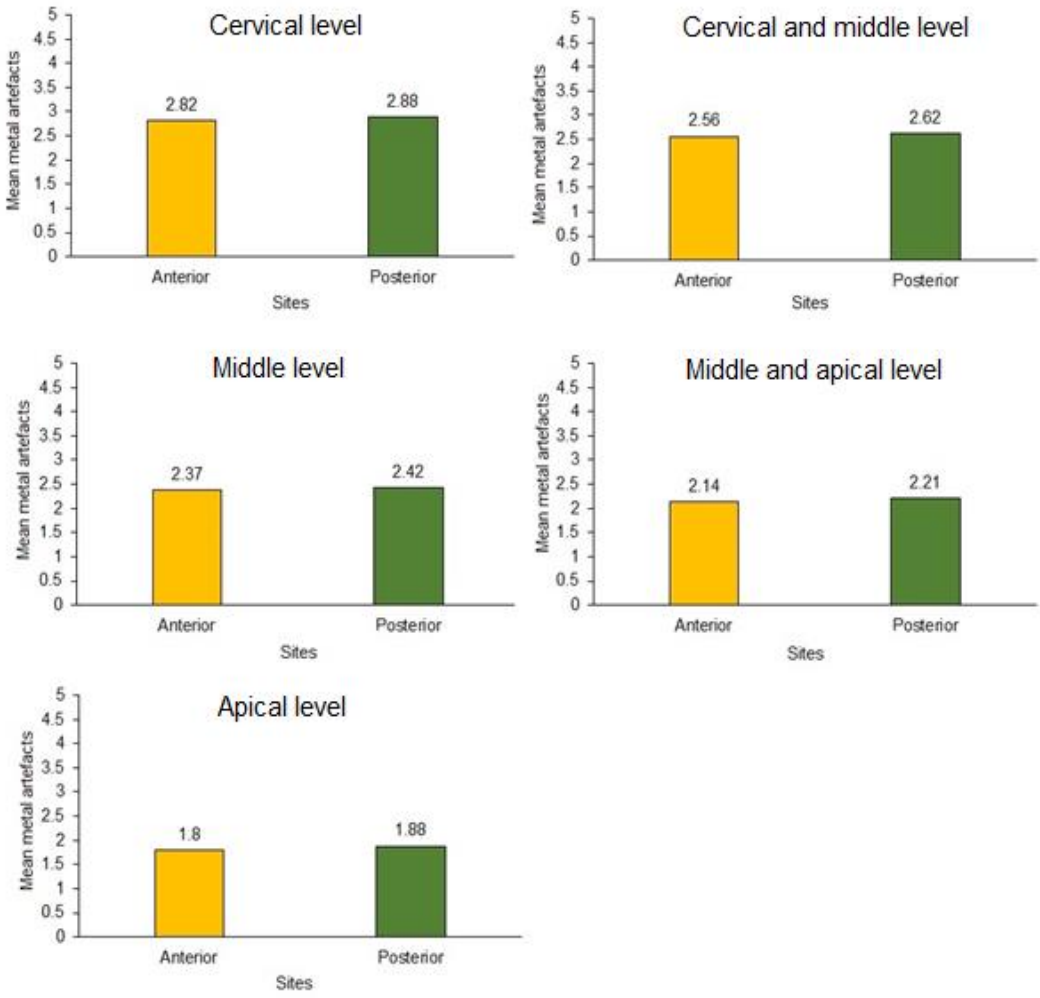

Figure 4: Column charts showing comparison of metal artefacts between anterior region of maxilla and mandible and posterior region of maxilla and mandible.

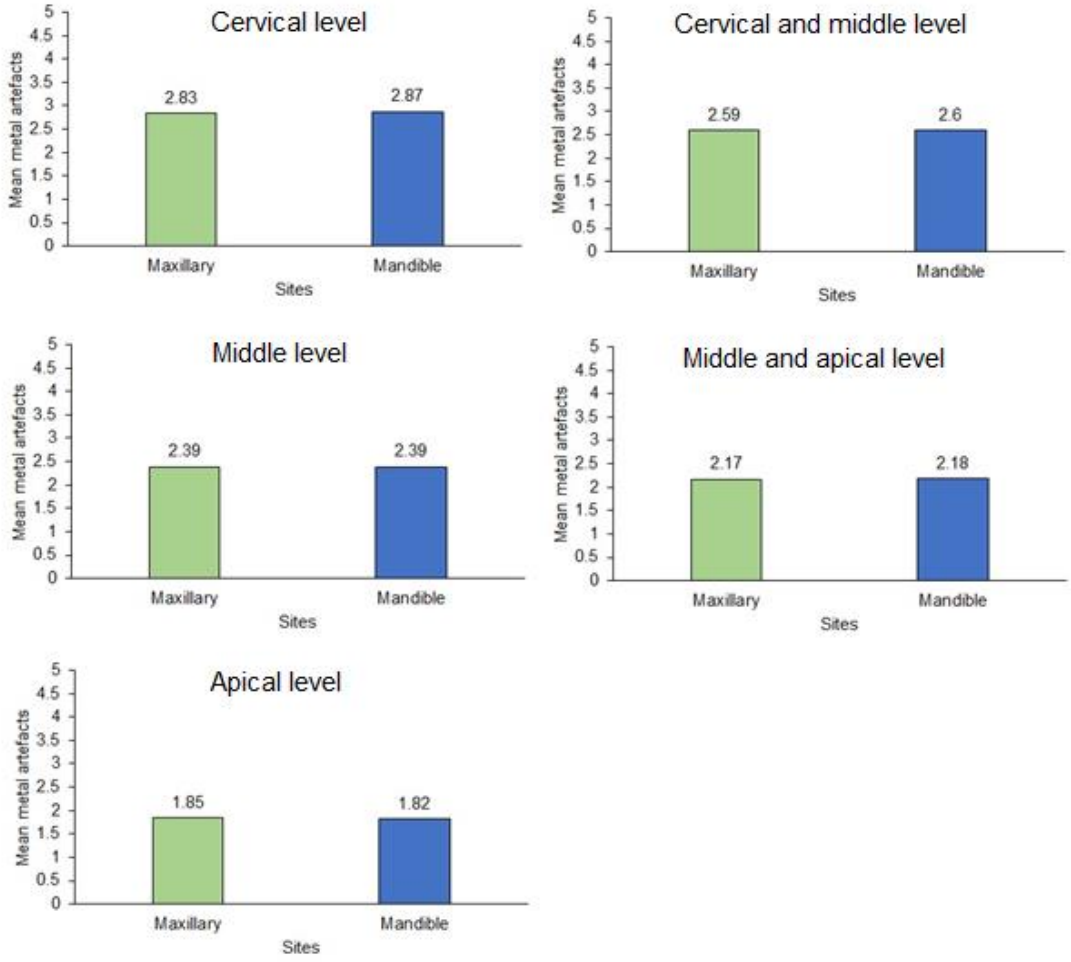

Figure 5: Column charts showing mean of metal artefacts in percentage between maxilla and mandible irrespective of anterior and posterior region.

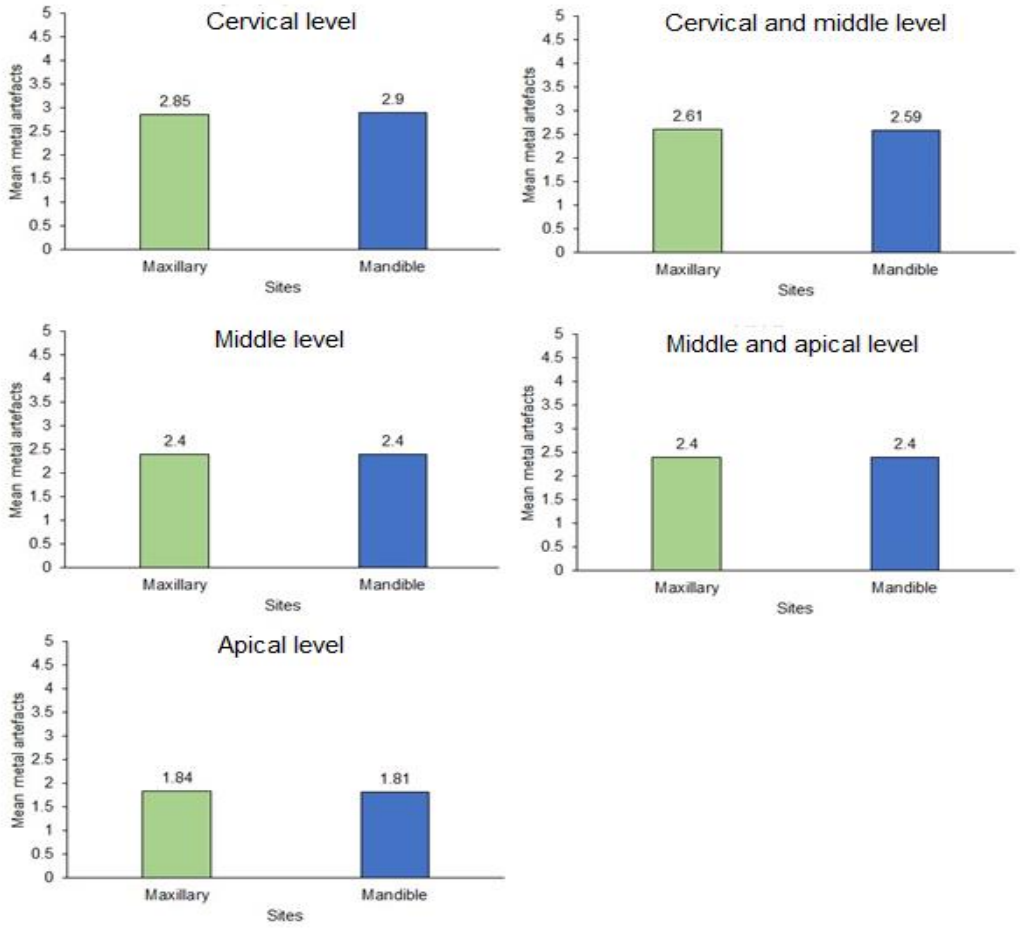

Figure 6: Column charts showing mean of metal artefacts in percentage between isolated implants of maxilla and mandible.

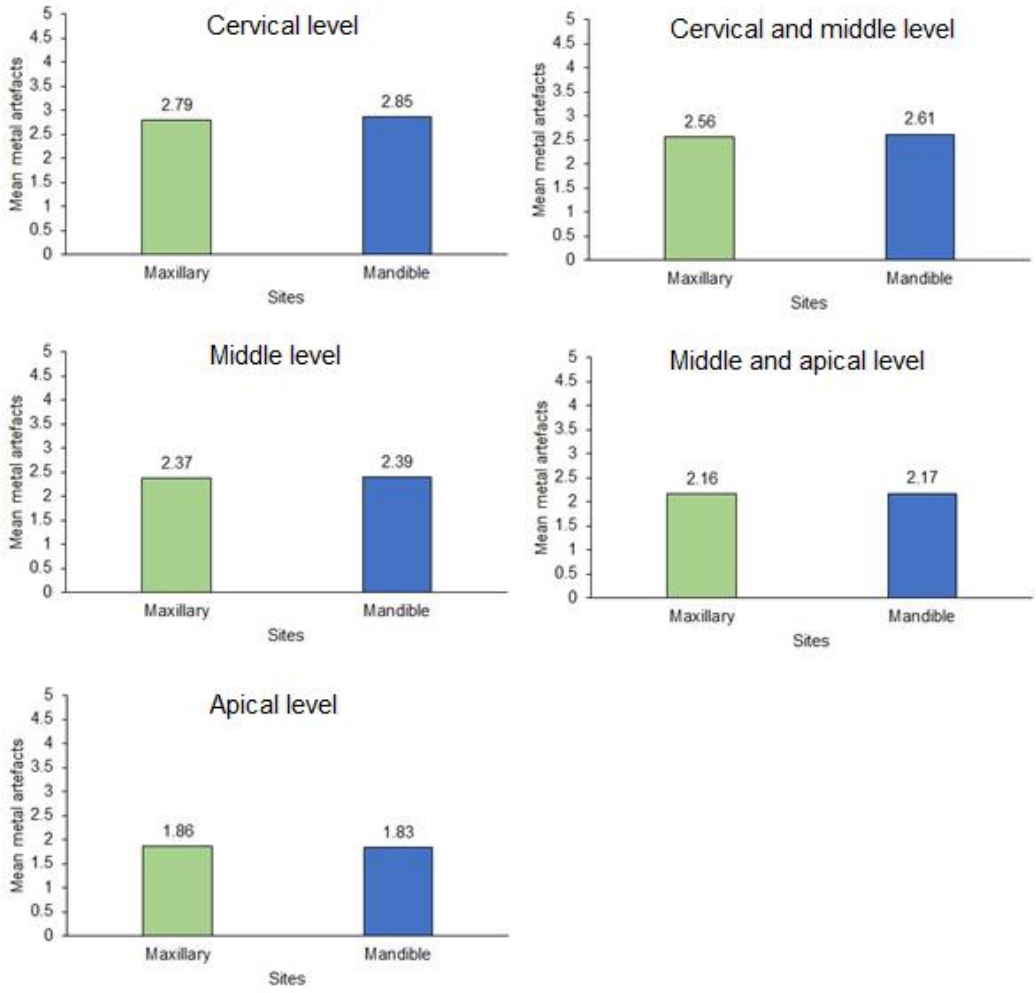

Figure 7: Column charts showing mean of metal artefacts in percentage between adjacent implants of maxilla and mandible.

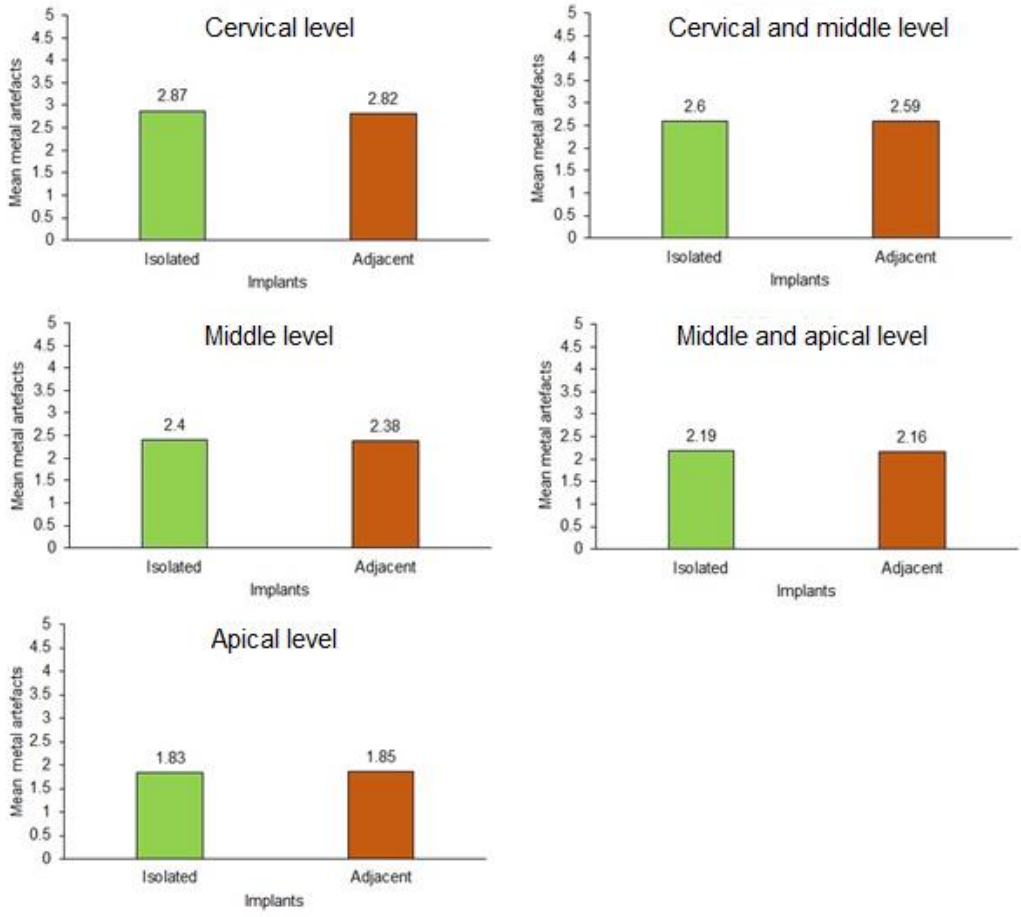

Figure 8: Column charts showing mean of metal artefacts in percentage between isolated and adjacent implants.

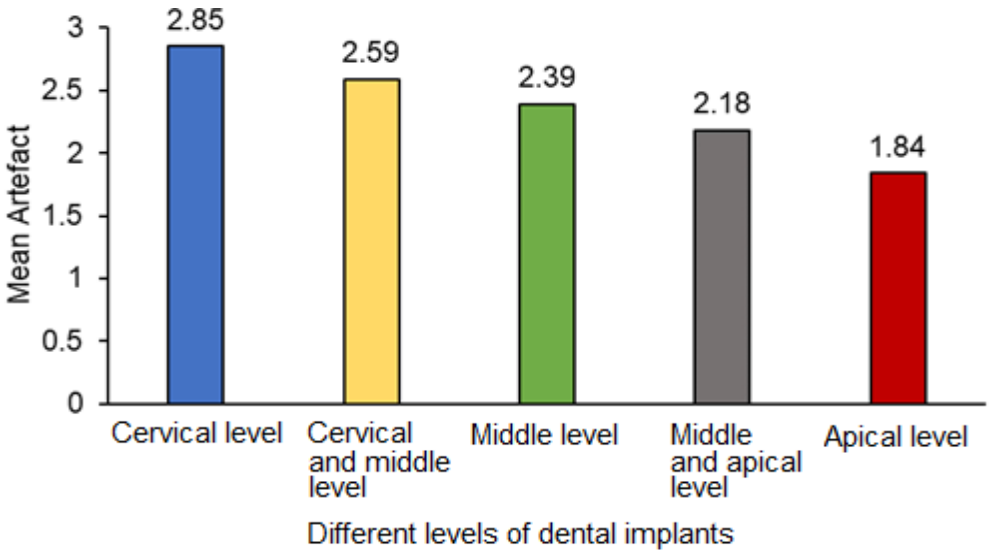

Figure 9: Column chart showing comparison of metal artefacts in percentage across 5 different levels of dental implants.

CASE HISTORY PROFORMA

Name:

Age/ Gender:

Implant site:

Group	**Implant**		**Percentage of metal artefacts at 5 different levels of implants**				
	Isolated Implant	**Adjacent implant**	**Level 1**	**Level 2**	**Level 3**	**Level 4**	**Level 5**

$$\text{Artefact quantification (\%)} = \frac{\text{Actual SD}}{\text{Theoretical maximum SD}} \times 100$$

Master chart

Group I —Included 26 Implants placed in anterior maxilla;

Group II —Included 26 Implants placed in posterior maxilla;

Group III —Included 26 Implants placed in anterior mandible;

Group IV —Included 26 Implants placed in posterior mandible.

Level 1 - Cervical level

Level 2 – Between cervical and middle

Level 3 - Middle level

Level 4 – Between middle and apical

Level 5 – Apical level

		Implant		Percentage of metal artefact at 5 different levels of implants				
Sr.nos	Group	Isolated Implant	Adjacent Implant	Level 1	Level 2	Level 3	Level 4	Level 5
1	Group I	Isolated		2.9	2.7	2.5	2.3	1.8
2	Group I	Isolated		2.7	2.5	2.3	2.0	1.7
3	Group I	Isolated		2.9	2.7	2.5	2.3	1.9
4	Group I	Isolated		2.6	2.5	2.5	2.2	1.6
5	Group I	Isolated		3.0	2.7	2.5	2.3	1.9
6	Group I		Adjacent	2.7	2.5	2.3	2.2	1.8
7	Group I		Adjacent	2.6	2.4	2.2	2.1	1.7
8	Group I	Isolated		3.0	2.6	2.4	2.2	1.8
9	Group I	Isolated		2.9	2.5	2.3	2.2	1.9
10	Group I	Isolated		3.0	2.7	2.5	2.3	1.9
11	Group I	Isolated		2.8	2.5	2.3	2.1	1.8
12	Group I		Adjacent	2.7	2.4	2.3	2.1	1.8
13	Group I	Isolated		2.8	2.4	2.2	2.0	1.7
14	Group I		Adjacent	3.0	2.5	2.3	2.0	1.9
15	Group I		Adjacent	2.7	2.5	2.3	2.0	1.8
16	Group I		Adjacent	2.8	2.5	2.3	2.0	1.7
17	Group I	Isolated		2.6	2.5	2.4	2.0	1.6
18	Group I	Isolated		2.6	2.4	2.3	2.1	1.9
19	Group I	Isolated		2.9	2.6	2.3	2.1	1.8
20	Group I		Adjacent	2.6	2.4	2.3	2.0	1.7
21	Group I		Adjacent	2.7	2.5	2.3	2.1	1.9
22	Group I	Isolated		2.9	2.6	2.4	2.2	1.9
23	Group I		Adjacent	2.7	2.5	2.3	2.2	1.8

24	Group I		Adjacent	2.7	2.5	2.3	2.0	1.9
25	Group I	Isolated		2.6	2.4	2.2	2.1	1.8
26	Group I		Adjacent	3.0	2.7	2.4	2.2	1.9
1	Group II	Isolated		2.9	2.7	2.5	2.3	1.9
2	Group II	Isolated		3.0	2.8	2.4	2.2	1.8
3	Group II		Adjacent	2.9	2.7	2.5	2.3	2.0
4	Group II	Isolated		2.9	2.8	2.7	2.5	2.1
5	Group II	Isolated		2.6	2.4	2.0	1.8	1.6
6	Group II	Isolated		2.9	2.7	2.5	2.3	1.8
7	Group II	Isolated		2.8	2.6	2.4	2.2	1.8
8	Group II		Adjacent	2.6	2.5	2.3	2.1	1.8
9	Group II		Adjacent	2.8	2.5	2.3	2.1	1.9
10	Group II	Isolated		3.1	2.6	2.4	2.2	1.9
11	Group II		Adjacent	2.9	2.7	2.6	2.3	1.8
12	Group II		Adjacent	2.8	2.6	2.4	2.2	1.9
13	Group II	Isolated		3.0	2.7	2.5	2.2	2.1
14	Group II	Isolated		2.9	2.7	2.5	2.3	1.9
15	Group II	Isolated		2.8	2.6	2.4	2.2	1.8
16	Group II		Adjacent	2.6	2.5	2.4	2.2	2.0
17	Group II		Adjacent	2.9	2.7	2.5	2.3	1.9
18	Group II		Adjacent	2.9	2.7	2.5	2.3	1.9
19	Group II		Adjacent	3.0	2.7	2.5	2.3	2.0
20	Group II	Isolated		2.9	2.7	2.5	2.2	1.9
21	Group II	Isolated		3.0	2.6	2.4	2.2	2.0
22	Group II	Isolated		2.9	2.7	2.4	2.1	1.9
23	Group II		Adjacent	2.8	2.6	2.4	2.2	1.8
24	Group II		Adjacent	2.9	2.7	2.5	2.3	2.1
25	Group II	Isolated		2.8	2.6	2.4	2.2	1.9
26	Group II	Isolated		2.9	2.7	2.5	2.3	1.9
								`
1	Group III		Adjacent	2.7	2.4	2.2	2.0	1.8
2	Group III	Isolated		3.0	2.7	2.5	2.3	1.9
3	Group III		Adjacent	3.1	2.8	2.6	2.4	2.0
4	Group III	Isolated		2.7	2.4	2.1	1.9	1.4
5	Group III		Adjacent	2.6	2.5	2.3	2.1	1.8
6	Group III		Adjacent	2.9	2.7	2.5	2.3	1.9
7	Group III		Adjacent	2.5	2.3	2.1	1.9	1.6
8	Group III	Isolated		2.6	2.4	2.2	2.0	1.7
9	Group III		Adjacent	2.7	2.5	2.3	2.0	1.4
10	Group III	Isolated		3.1	2.8	2.6	2.4	2.0
11	Group III	Isolated		3.0	2.7	2.5	2.3	1.9
12	Group III		Adjacent	2.7	2.5	2.3	2.1	1.8
13	Group III	Isolated		2.7	2.4	2.2	2.0	1.6
14	Group III		Adjacent	2.9	2.6	2.4	2.2	1.9
15	Group III		Adjacent	3.1	2.8	2.6	2.3	2.0

16	Group III		Adjacent	3.0	2.7	2.5	2.3	1.9
17	Group III		Adjacent	2.9	2.6	2.4	2.2	1.9
18	Group III		Adjacent	2.6	2.4	2.2	2.0	1.6
19	Group III		Adjacent	3.2	2.7	2.5	2.2	1.8
20	Group III		Adjacent	2.7	2.6	2.3	2.1	1.7
21	Group III		Adjacent	3.1	2.8	2.6	2.2	1.8
22	Group III	Isolated		3.0	2.8	2.6	2.3	1.9
23	Group III	Isolated		2.6	2.4	2.2	2.0	1.7
24	Group III	Isolated		2.6	2.5	2.3	2.1	1.7
25	Group III	Isolated		3.0	2.8	2.5	2.3	1.9
26	Group III	Isolated		3.2	2.8	2.6	2.3	2.0
1	Group IV	Isolated		3.1	2.8	2.7	2.5	1.9
2	Group IV	Isolated		2.9	2.7	2.5	2.3	2.0
3	Group IV	Isolated		3.3	2.7	2.6	2.4	1.9
4	Group IV	Isolated		2.5	2.4	2.3	2.1	1.6
5	Group IV	Isolated		2.9	2.5	2.2	2.1	1.7
6	Group IV	Isolated		3.0	2.4	2.2	2.1	2.0
7	Group IV	Isolated		2.9	2.6	2.3	2.2	1.9
8	Group IV	Isolated		3.1	2.7	2.5	2.2	1.7
9	Group IV	Isolated		3.1	2.5	2.7	2.2	1.7
10	Group IV	Isolated		2.8	2.6	2.4	2.1	1.8
11	Group IV		Adjacent	2.8	2.6	2.2	2.1	2.0
12	Group IV		Adjacent	2.8	2.5	2.4	2.2	1.8
13	Group IV		Adjacent	3.0	2.7	2.5	2.2	2.1
14	Group IV		Adjacent	2.8	2.6	2.4	2.1	1.6
15	Group IV		Adjacent	2.5	2.4	2.3	2.2	1.9
16	Group IV		Adjacent	3.0	2.5	2.4	2.1	1.9
17	Group IV		Adjacent	2.8	2.6	2.3	2.1	1.7
18	Group IV	Isolated		2.7	2.5	2.3	2.0	1.8
19	Group IV		Adjacent	2.9	2.8	2.4	2.4	2.3
20	Group IV		Adjacent	2.8	2.6	2.4	2.1	1.8
21	Group IV		Adjacent	2.9	2.6	2.4	2.2	2.0
22	Group IV		Adjacent	2.9	2.7	2.4	2.2	1.6
23	Group IV		Adjacent	3.0	2.8	2.4	2.2	1.8
24	Group IV		Adjacent	2.9	2.7	2.5	2.3	1.9
25	Group IV	Isolated		2.9	2.4	2.3	2.2	1.9
26	Group IV	Isolated		2.9	2.6	2.4	2.2	1.8